Enhanced Arctic-Tethys connectivity ended the Toarcian Oceanic Anoxic Event in NW Europe

B. van de Schootbrugge[1] ⬤, A. J. P. Houben[2], F. E. Z. Ercan[1], R. Verreussel[2], S. Kersholt[2], N. M. M. Janssen[2], B. Nikitenko[3,4] and G. Suan[5]

[1]Utrecht University, Marine Palynology & Paleoceanography Group, Department of Earth Sciences, Princetonlaan 8A, 3584 CS Utrecht, The Netherlands; [2]Geological Survey of the Netherlands-TNO, Princetonlaan 6, 3584CB, Utrecht, The Netherlands; [3]Institute of Petroleum Geology and Geophysics, Siberian Branch of Russian Academy of Sciences, Ac. Koptyg ave. 3, Novosibirsk 90, RU-630090, Russia; [4]Novosibirsk State University, Pirogova str.1, Novosibirsk 90, 630090, Russia and [5]UMR CNRS 5276 LGLTPE, Université Lyon 1, École Normale Supérieure de Lyon, Villeurbanne Cedex, France

Abstract

The Toarcian Oceanic Anoxic Event (T-OAE, *c.* 182 Ma) represents a major perturbation of the carbon cycle marked by widespread black shale deposition. Consequently, the onset of the T-OAE has been linked to the combined effects of global warming, high productivity, basin restriction and salinity stratification. However, the processes that led to termination of the event remain elusive. Here, we present palynological data from Arctic Siberia (Russia), the Viking Corridor (offshore Norway) and the Yorkshire Coast (UK), all spanning the upper Pliensbachian – upper Toarcian stages. Rather than a 'dinoflagellate cyst black-out', as recorded in T-OAE strata of NW Europe, both the Arctic and Viking Corridor records show high abundance and dinoflagellate diversity throughout the T-OAE interval as calibrated by C-isotope records. Significantly, in the Arctic Sea and Viking Corridor, numerous species of the *Parvocysta* and *Phallocysta* suites make their first appearance in the lower Toarcian Falciferum Zone much earlier than in Europe, where these key dinoflagellate species appeared suddenly during the Bifrons Zone. Our results indicate migrations of Arctic dinoflagellate species, driven by relative sea-level rise in the Viking Corridor and the establishment of a S-directed circulation from the Arctic Sea into the Tethys Ocean. The results support oceanographic models, but are at odds with some interpretations based on geochemical proxies. The migration of Arctic dinoflagellate species coincides with the end of the T-OAE and marks the arrival of oxygenated, low-salinity Arctic waters, triggering a regime change from persistent euxinia to more dynamic oxygen conditions.

1. Introduction

The Toarcian Oceanic Anoxic Event (T-OAE) is generally regarded as a global, short-lived perturbation of the carbon cycle that occurred during the Exaratum Subzone of the Falciferum Zone (Jenkyns, 1988; Hesselbo *et al.* 2000; Suan *et al.* 2008b; Boulila *et al.* 2014) (Fig. 1). It is marked by a negative carbon isotope excursion (CIE) of around 3–4 per mille in both carbonate and organic carbon substrates (Suan *et al.* 2015), which has been documented in many locations in Europe (Sabatino *et al.* 2009, 2013; Kafousia *et al.* 2011), as well as in NW Africa (Bodin *et al.* 2016), North and South America (Al-Suwaidi *et al.* 2010; Martindale *et al.* 2017), Siberia (Suan *et al.* 2011) and Japan (Izumi *et al.* 2012). In many localities, laminated black shales were deposited during this time interval with lipid-rich (high hydrogen index) and high total organic carbon (TOC) values and abundant green algal organic matter. Biomarkers indicating photic zone euxinia (Schouten *et al.* 2000; Frimmel *et al.* 2004; Ruebsam *et al.* 2018) provide evidence for strong water column stratification at the zenith of the carbon cycle perturbation (van de Schootbrugge *et al.* 2013).

In Europe, Toarcian black shales formed in response to the interplay between four main factors with strong feedback links: (1) temperature reconstructions based on belemnite and brachiopod calcite document a substantial (> 7°C) temperature increase of ocean waters at the onset of the Toarcian OAE (Bailey *et al.* 2003; Rosales *et al.* 2004; van de Schootbrugge *et al.* 2005; Suan *et al.* 2008a; Korte *et al.* 2015), making greenhouse warming a likely contributor to ocean deoxygenation; (2) ocean deoxygenation was regionally exacerbated by elevated rates of marine organic matter production, mainly driven by green algal primary producers, cyanobacteria, and secondary microbial producers, such as sulphur bacteria, leading to bottom water anoxia and photic zone euxinia (Bucefalo Palliani *et al.* 2002; van de Schootbrugge *et al.* 2013); (3) greenhouse warming also increased stratification of the water column, leading to extremely slow mixing of deeper waters, further enhancing oxygen depletion (McArthur *et al.* 2008); and (4) circulation was further impeded by elevated run-off from continental

landmasses (Cohen *et al.* 2004; Dera *et al.* 2009a; Them *et al.* 2017) altering surface water salinity and delivering essential nutrients to fuel primary production (Montero-Serrano *et al.* 2015; Xu *et al.* 2018).

When the geographic distribution of black shales in epicontental NW European marine basins is taken into account, it becomes clear that ocean circulation also played a significant role in driving spatial differences in anoxia (Harazim *et al.* 2013). In sections close to the palaeo-equator, for example in Portugal (Da Rocha *et al.* 2016) and Morocco (Bodin *et al.* 2010), no black shales formed; however, further north in the UK and Germany, TOC values drastically increase and, in some basins, black shale deposition continued throughout the Toarcian Age, well beyond the immediate negative CIE. For example, in the Grands Causses Basin in southern France, sediment deposition continued in anoxic facies following the Schistes Cartons Formation (Harazim *et al.* 2013), while in Germany upper Toarcian paper shales are largely indistinguishable from those of the lower Toarcian (van de Schootbrugge *et al.* 2018).

Regional differences in the intensity of organic matter deposition as well as the prolongation of anoxia in some parts of the European Epicontinental Seaway (EES) were mainly driven by reorganizations in ocean circulation. Connections with the Arctic Sea through the Viking Corridor and circulation within the Tethys Ocean likely played particularly important roles in oxygenation, stratification and isolation of basins across the EES (Dera & Donnadieu, 2012). However, different authors have arrived at very different conclusions regarding the importance, timing, direction and intensity of flow through the Viking Corridor, with major implications for our understanding of biotic and chemical evolution during the Pliensbachian–Toarcian interval. Prauss & Riegel (1989) were the first to advocate a significant role for the influx of low-salinity Arctic waters to drive density stratification during the early Toarcian Age, using mainly the abundance of prasinophyte green algae in the EES and their presumed cold-water, low-salinity affinity. Bjerrum & Surlyk (2001) used numerical modelling to suggest that flow through the Viking Corridor was mainly directed southwards. Their model was supported by Dera *et al.* (2009b) based on sparse Nd-isotope data. In contrast, from a compilation of oxygen isotope data Korte *et al.* (2015) deduced that flow was mainly northwards for the entire duration of the Toarcian Age and that tectonic movements led to a shutdown of warm water flow only during the Aalenian Age, triggering cooling in the northern high latitudes. More recently, Ruvalcaba Baroni *et al.* (2018) used trace-element data and coupled ocean–atmosphere model runs to argue for strong clockwise currents in the Tethys and complex bathymetry in the EES as important factors in determining regional oxygenation.

In addition to geochemical proxy records, water mass exchange between basins can be studied in great detail using the stratigraphic distribution of nektonic, planktonic and benthic fossil groups such as ammonites, bivalves or microfossils. Here, we examine dinoflagellate cyst records from sections strategically situated at the northern end (Siberia, Russia), and within (offshore Norway) and at the southern end of the Viking Corridor (Yorkshire, UK). Phytoplankton, eukaryotic single-celled algae that float with the currents, are sensitive tracers of water mass conditions, including temperature, salinity and redox state controlling nutrient availability. In general, tolerance of phytoplankton taxa for temperature and salinity variations is larger than for macro-organisms such as cephalopods; phytoplankton therefore respond quicker to opening gateways. As such, palynology provides a powerful tool to trace changes in oceanography, as has been shown for other (oceanic anoxic) events (Vellekoop *et al.* 2015; van Helmond *et al.* 2016).

Prauss (1989), Prauss & Riegel (1989) and Prauss *et al.* (1991) suggested that Toarcian and Aalenian–Bajocian cyst-producing dinoflagellate diversity in NW Europe was mainly determined by sea-level changes that allowed for exchange between the Arctic and the Tethys. This view has been echoed in later work by Riding, Bucefalo Palliani and Poulsen. However, all these authors were limited by the fact that all the data to support oceanographic models derived from NW Europe. Here, we present for the first time robust stratigraphic dinoflagellate cyst data from both ends of the Viking Corridor.

2. Geological background

To trace ocean circulation between the Arctic Sea and Tethys Ocean through the Viking Corridor (Figs 1, 2) we use the spatial and temporal distribution of Early Jurassic dinoflagellate cysts and present new data for the Kelimyar River S16 and Kelimyar River S5-D1 sections (Fig. 3) in the Olenek River area (Arctic part of Eastern Siberia, Russia; Fig. 1). We compare our data from Siberia with records from within the Viking Corridor from the northern part of the North Sea offshore Norway (Core 34/10-35 from an exploration well in the Gullfaks South Field) using bulk organic carbon isotopes for correlation. Tracing dinoflagellate migrations further south, we use new palynological and carbon isotope data from a key composite section of exposures along the Yorkshire coast (Cleveland Basin, UK; Fig. 1). We compare/integrate our new data with previously published accounts of quantitative and qualitative dinoflagellate records from high- and low-latitude sites.

Along the Yorkshire Coast (UK), between the town of Staithes in the north down to the hamlet of Ravenscar in the south, the Lower Jurassic sequence of the Cleveland Basin is exposed in the coastal cliffs, in several partially repetitive outcrops (see Howard, 1985; Hesselbo & Jenkyns, 1995; Simms *et al.* 2004). The Lower Jurassic succession of the Cleveland Basin is dominated by mudrocks. An abundance of ammonites has long enabled this lithostratigraphical framework to be tied in precisely to the ammonite biostratigraphy for the Lower Jurassic sequence.

We have sampled the Pliensbachian–Toarcian succession (Staithes Sandstone, Cleveland Ironstone, Whitby Mudstone and Blea Wyke Sandstone formations) at various locations between Staithes and Runswick Bay and near Kettleness. The upper Toarcian succession was sampled SE of the Peak Fault near Ravenscar. The Staithes Sandstone Formation is approximately 25 m thick, and is dominated by tempestitic sandstones and siltstones. It extends up into the Margaritatus Zone and spans the Capricornus, Figulinum and Stokesi subzones. The Cleveland Ironstone Formation, encompassing the remainder of the Margaritatus Zone and the entire Spinatum Zone, is characterized by silty mudstone coarsening-upward cycles capped by oolitic ironstones. The base of the overlying Whitby Mudstone Formation is taken at a rapid upwards change to mudstone and is coincident with the Pliensbachian–Toarcian boundary (Simms *et al.* 2004). The Whitby Mudstone Formation is characterized by a dark, more than 100-m-thick mudstone-dominated succession. It is divided into five members, commencing with the silty mudstones and calcareous or sideritic nodule bands of the Grey Shale Member, passing through the predominantly bituminous shales of the Mulgrave Shale and Alum Shale members, before passing back into silty mudstones of the Peak Mudstone Member and finally the still more silty Fox Cliff Siltstone Member (Simms *et al.* 2004). The Jet Rock contains the negative CIE of the Toarcian Oceanic Anoxic Event (Fig. 4) and has substantially elevated organic carbon
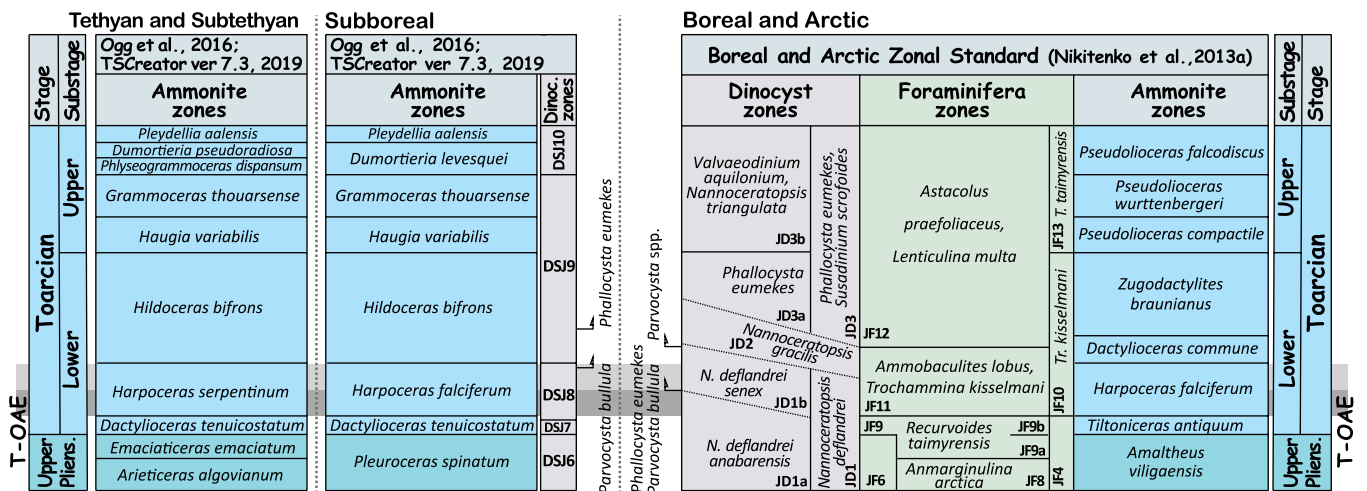
Tethyan and Subtethyan

Stage	Substage	Ammonite zones (Ogg et al., 2016; TSCreator ver 7.3, 2019)
Toarcian	Upper	*Pleydellia aalensis*
		Dumortieria pseudoradiosa
		Phlyseogrammoceras dispansum
		Grammoceras thouarsense
		Haugia variabilis
	Lower	*Hildoceras bifrons*
		Harpoceras serpentinum
		Dactylioceras tenuicostatum
Upper Pliens.		*Emaciaticeras emaciatum*
		Arieticeras algovianum

Subboreal

Ammonite zones (Ogg et al., 2016; TSCreator ver 7.3, 2019)	Dinoc. zones
Pleydellia aalensis	DSJ10
Dumortieria levesquei	
Grammoceras thouarsense	DSJ9
Haugia variabilis	
Hildoceras bifrons	
Harpoceras falciferum	DSJ8
Dactylioceras tenuicostatum	DSJ7
Pleuroceras spinatum	DSJ6

Phallocysta eumekes — *Parvocysta* spp.
Parvocysta bullula
Phallocysta eumekes Parvocysta bullula

Boreal and Arctic

Boreal and Arctic Zonal Standard (Nikitenko et al., 2013a)

Dinocyst zones		Foraminifera zones		Ammonite zones		Substage	Stage
Valvaeodinium aquilonium, Nannoceratopsis triangulata JD3b	*Phallocysta eumekes, Susadinium scrofoides* JD3	*Astacolus praefoliaceus, Lenticulina multa*	JF13 *T. taimyrensis*	*Pseudolioceras falcodiscus*		Upper	Toarcian
				Pseudolioceras wurttenbergeri			
Phallocysta eumekes JD3a				*Pseudolioceras compactile*			
Nannoceratopsis gracilis JD2		JF12	*Tr. kisselmani*	*Zugodactylites braunianus*	JF10		
N. deflandrei senex JD1b	*Nannoceratopsis deflandrei* JD1	*Ammobaculites lobus, Trochammina kisselmani* JF11		*Dactylioceras commune*		Lower	
				Harpoceras falciferum			
N. deflandrei anabarensis JD1a		JF9 *Recurvoides taimyrensis* JF9b		*Tiltoniceras antiquum*	JF4	Upper Pliens.	
		JF6 *Anmarginulina arctica* JF8	JF9a	*Amaltheus viligaensis*			

Fig. 1. Zonal subdivision of the uppermost Pliensbachian and Toarcian successions of the Tethyan and Sub-tethyan, sub-boreal, boreal and Arctic realms, and FO of some important species of the dinoflagellate cysts in the different palaeogeographical realms. Modified after Nikitenko et al. (2013b).
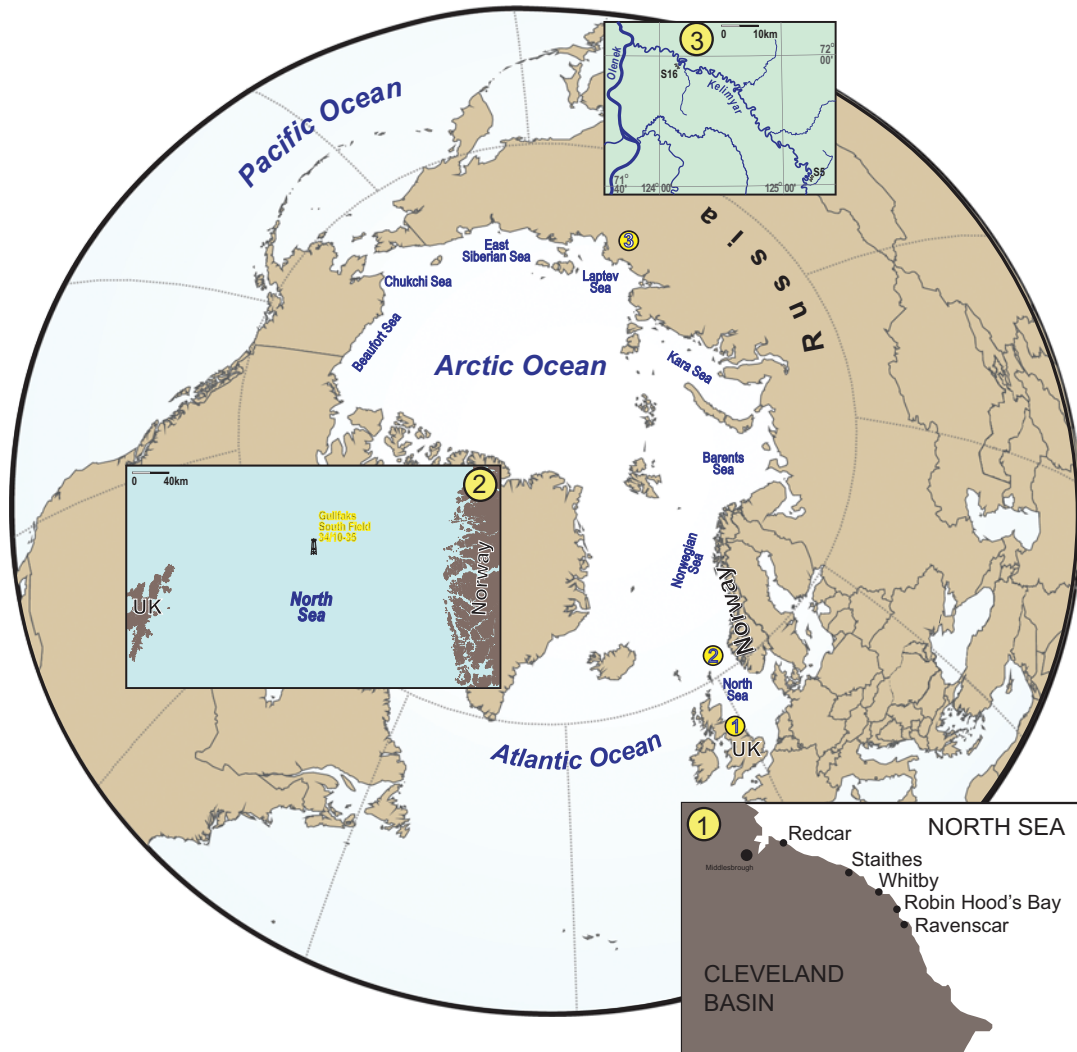

Fig. 2. Current geography and detailed maps for the investigated locations: (1) Kelimyar River, Siberia, Russia; (2) Gulfaks oil field offshore Norway; and (3) Yorkshire, UK.
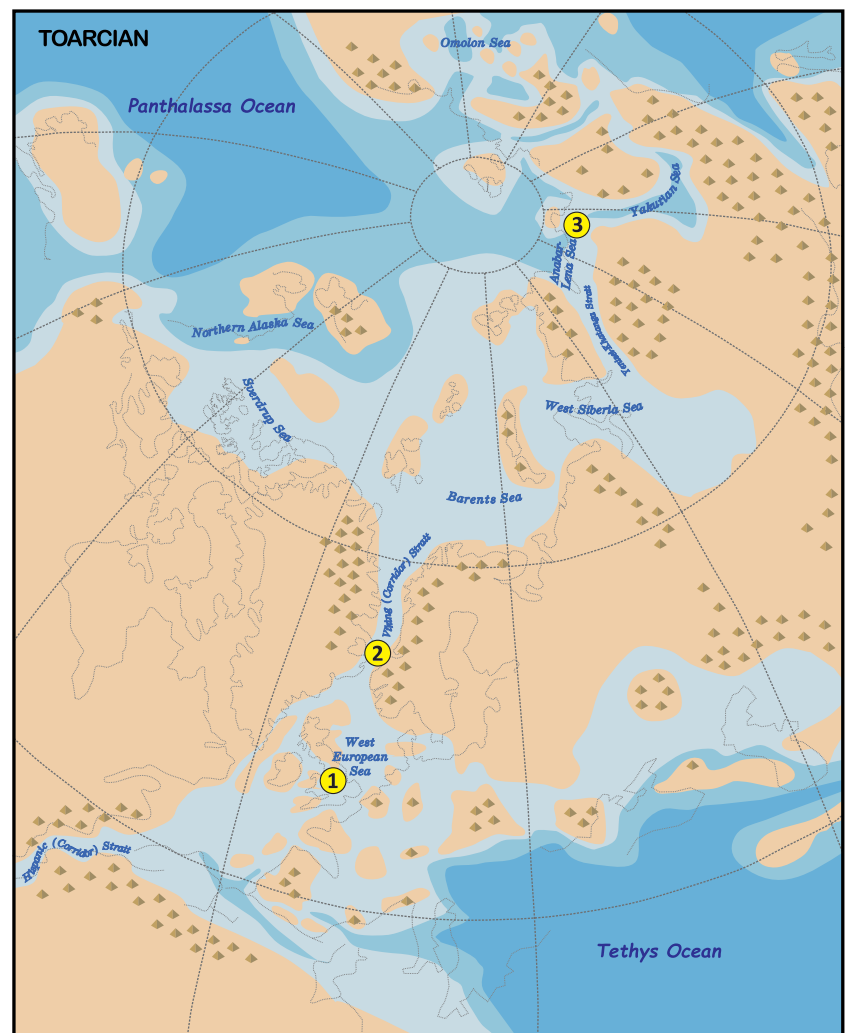
Fig. 3. Palaeogeographic reconstruction for the Toarcian Stage (182 Ma) using G-Plates. Plate tectonic reconstructions after Scotese (2016) with modifications; Arctic palaeogeography reconstructions after Nikitenko & Mickey (2004) with modifications. 1, Yorkshire Coast, Cleveland Basin (UK); 2, Gulfaks 34/10-35S core (offshore Norway); and 3, Kelimyar River (Russia).

contents. Above the Whitby Mudstone Formation, the overlying Blea Wyke Sandstone Formation at the top of the Toarcian Stage, encompasses much of the Dispansum and Pseudoradiosa zones. It is divided into the Grey Sandstone Member, of muddy micaceous siltstone or fine sandstone, and the overlying and somewhat coarser Yellow Sandstone Member. However, across much of the Cleveland Basin the upper part of the Toarcian succession is absent, with the base of the Dogger Formation (Middle Jurassic) resting unconformably upon various levels in the Alum Shale Member. Only to the SE of the Peak Fault, as at Blea Wyke in the Peak Trough, are these higher Toarcian units preserved.

From the Cleveland Basin, we analyzed 72 samples for palynology. Because of the lithological distinction among units and the various concretionary marker beds, we were able to accurately correlate the Grey Shales to Jet Rock interval to the bulk-organic carbon isotope curves of Kemp *et al.* (2005, 2011) and Littler *et al.* (2010). We therefore adopt their bulk organic carbon isotope dataset between 210 and 236 m composite position. The remainder of the Pliensbachian–Toarcian carbon isotope is new.

Records from within the Viking Corridor can only be studied through boreholes. Here, we present marine palynological and organic carbon isotope data from Well 34/10-35 (Fig. 5), which was drilled on the Tjalve Terrace SE of the Gullfaks South field in the northern North Sea (61° 4′ 16.17″ N and 2° 19′ 16.77″ E). The well was drilled in a water depth of 135 m and reached a total

depth of 4310 m in the lowermost Jurassic Statfjord Group. The main exploration targets were the sandstones of the Middle Jurassic Brent Group and the Pliensbachian–Toarcian Cook Formation, and therefore extensive cores were cut. Cores 1–11 cover the interval between 3931 and 4063.6 m measured depth (MD), and span the upper part of the Burton Formation, the Cook Formation and the Drake Formation. These lithostratigraphic interpretations are after the Norwegian Petroleum Directorate (NPD) Factpages (https://www.npd.no/en/facts/). The top of the investigated section reaches into the Middle Jurassic Brent Group. The lowermost part of the section (4063.6–4048 m MD) is characterized by grey, sandy to silty mudstones ascribed to the Burton Formation. The basal part (up to 4048 m MD) of the overlying Cook Formation is characterized by grey micaceous sandy shales that grade into light yellowish-brown fine carbonate-cemented hard micaceous sandstones (up to 3984 m MD). The transition to the overlying Drake Formation is not recovered by core and is positioned between 3970 and 3983 m MD. The Drake Formation here consists of olive black fissile slightly silty shale. The transition to the Brent Group (Ness Formation) is very sharp and unconformable at 3941.5 m MD. Based on palynostratigraphic data, the Cook Formation is inferred to be of Pliensbachian–Toarcian age (Vollset & Dore, 1984). Organic carbon isotope data required to constrain the position of the Toarcian CIE in the Cook–Drake sequence of
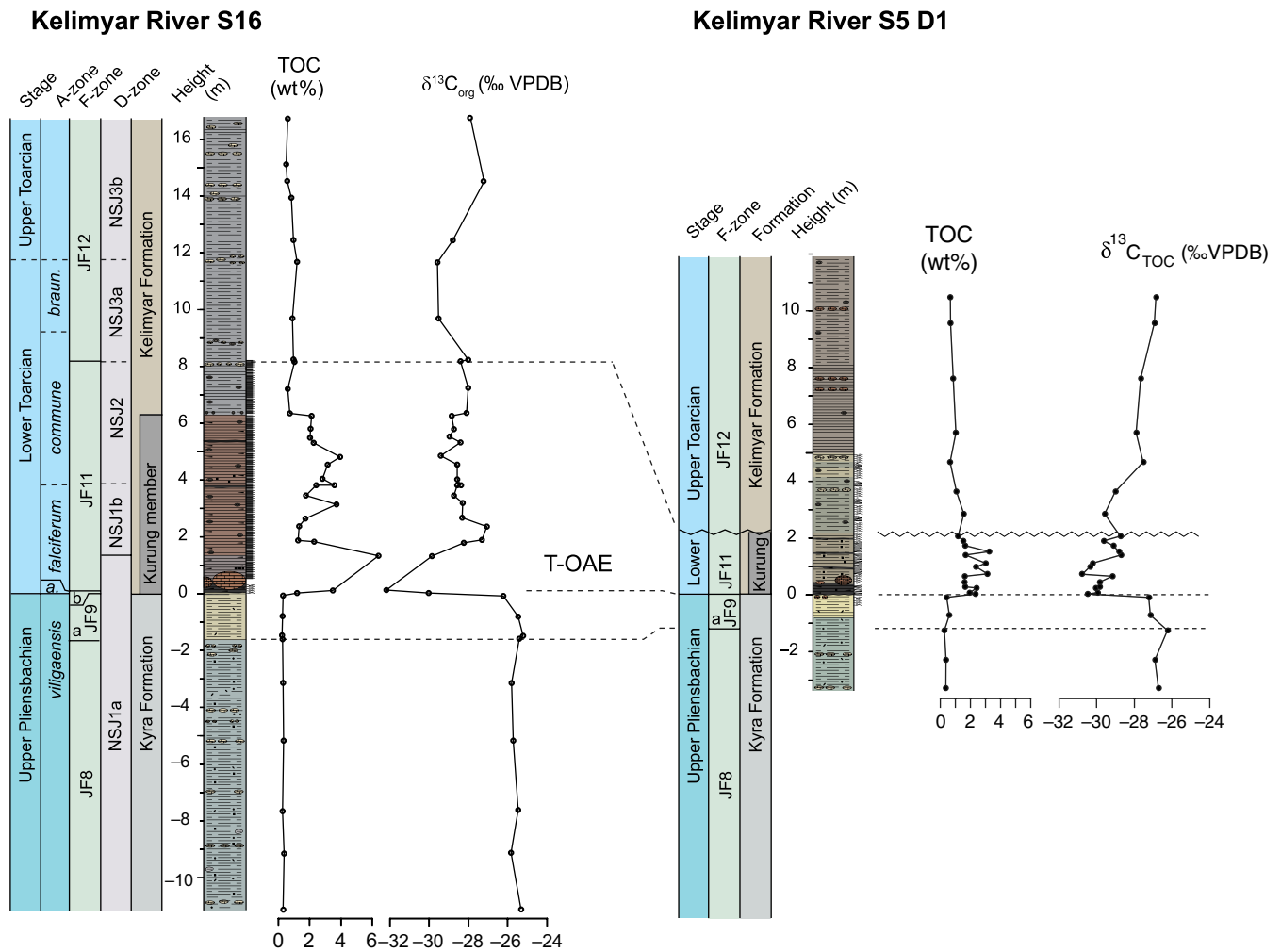
Fig. 4. Lithostratigraphy and geochemical proxy data for the Kelimyar River sections KR-S16 and KR-S5-D1 (modified from Suan *et al.* 2011).

the northern North Sea were previously unavailable. A total of 34 samples was therefore analysed for bulk organic carbon isotopic composition and total organic content. A total of 24 samples was processed and analysed for palynology.

The Kelimyar River S5-D1 section was studied by Devyatov *et al.* (2010) and Nikitenko *et al.* (2013a) for ammonites and foraminifera, and by Goryacheva (2017) for palynology. The section exposes the subsections Trench 1 and 2, the former being affected by a landslide in its upper part. In this study, the studied samples originate from the lower part of Trench 1 below the inferred landslide. In both sections KR-S16 and KR-S5-D1, the upper Pliensbachian Kyra Formation is dominated by siltstones and sandy siltstones with occasional rounded pebbles and gravels. These sediments were deposited in a shallow shelf setting that experienced episodic erosion during phases of low sea level. Benthic foraminifera indicate that the JF9 *Recurvoides taimyrensis* foraminiferal Zone (JF9b) is highly condensed and is missing entirely in section KR-S5 (Devyatov *et al.* 2010). In Siberia, this zone corresponds to the base of the Antiquum Zone (equivalent to the European Tenuicostatum Zone; Fig. 6). Accordingly, and considering previous palaeogeographic reconstructions of the Olenek River Basin, the succession exposed in KR-S5-D1 was likely deposited in a more proximal setting than that recorded in KR-S16. In both sections, the overlying lower Toarcian Kurung Member of the Kelimyar Formation is characterized by laminated black shales

with elevated TOC values (Suan *et al.* 2011; see also new KR-S5-D1 data in Fig. 3) and large concretions. The remainder of the Kelimyar Formation consists of siltstones and silty shales with small concretions and abundant belemnite rostra. Ammonites and benthic foraminifera indicate a late Toarcian age (Devyatov *et al.* 2010; Suan *et al.* 2011).

3. Methods

3.a. Palynology

Palynological processing for samples from Kelimyar River was performed both at the Goethe University Frankfurt (Germany) and Utrecht University (The Netherlands) using similar laboratory protocols for acid digestion, sieving and slide preparation. Samples were dried, and carbonate and silicate minerals were removed by reacting *c.* 10–20 g of small chips of sediment with concentrated HCl and HF in alternating steps, followed by neutralization with distilled water. To free individual palynomorphs from the large amounts of amorphous organic matter and pyrite that typically dominate Toarcian samples in the Siberian sections, additional treatment with Schultze's solution ($KClO_3$ + HNO_3) was performed. Sieving of samples occurred with a 15 micron mesh sieve. For the Siberian samples, permanent strew mounts were made using 'glue-for-glas', which is an ultraviolet (UV) light curing
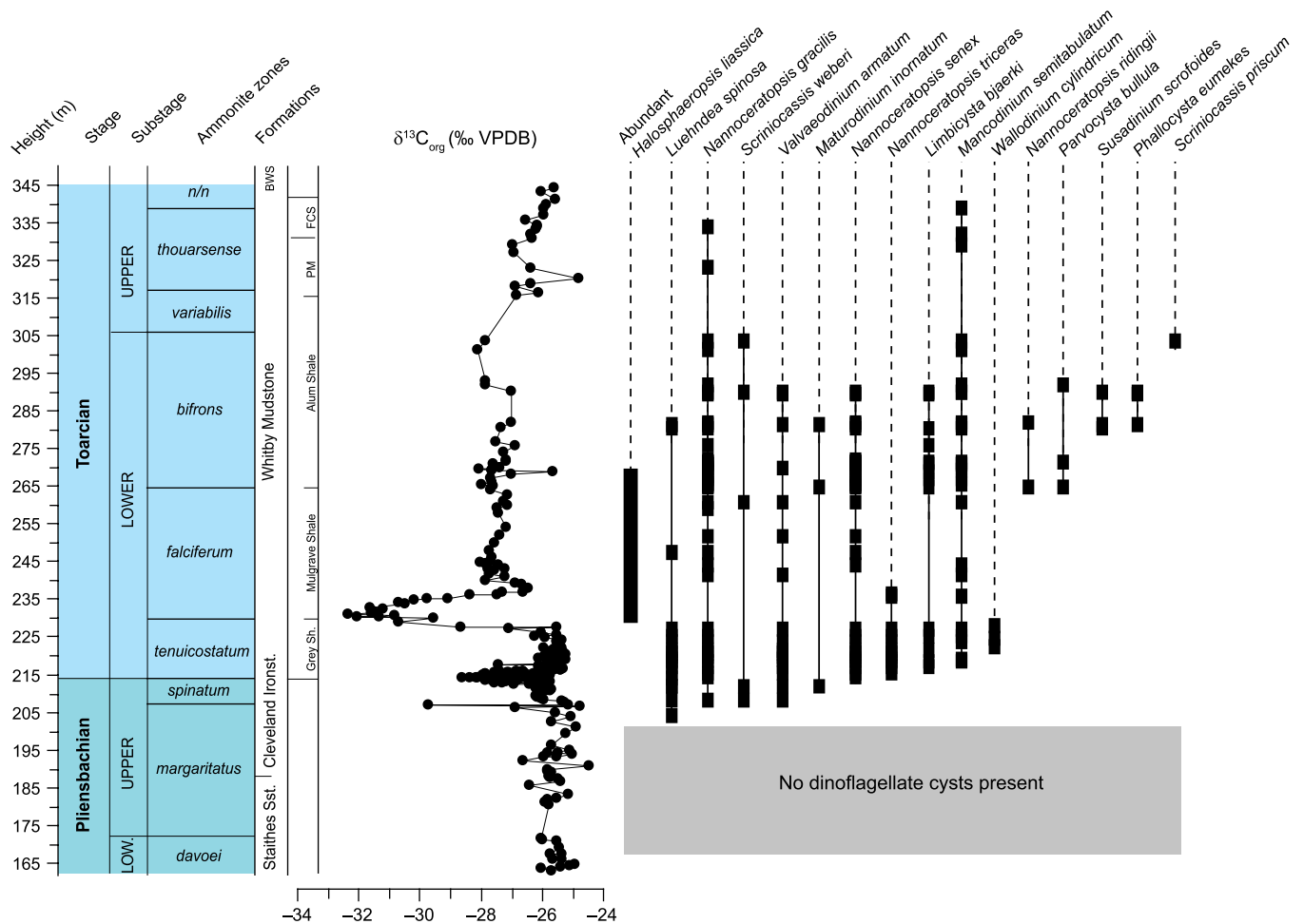
Fig. 5. Range chart and carbon isotope record for the Yorkshire Coast (Cleveland Basin, UK). The section is a composite (see geological background for a description of sampling locations).

adhesive. The samples from the Cleveland Basin and Well 34/10-35 were prepared at Utrecht University following a comparable protocol. Slides were prepared using the addition of glycerine jelly. For the Cleveland Basin dataset and for Well 34/10-35, UV-reflective microscopy was applied whenever large amounts of amorphous organic matter (AOM) hindered conventional optical analysis. Here, we only present range chart data for dinoflagellate cysts genera and species. Semiquantitative marine and terrestrial palynological records will be discussed in future work.

3.b. Geochemistry

Bulk organic carbon isotope data from Well 34/10-35 and the Cleveland Basin composite section were generated at Iso-Analytical Ltd based in Crewe (UK). Ratios were measured on a continuous-flow isotope ratio mass spectrometer (Europa Scientific 20-20 IRMS) with dual inlet, connected to an elemental analyser (EA-IRMS). Sample powders were pre-treated with 4 M HCl to remove any carbonate phases. Reproducibility, as determined via replicate measurements of 20% of the samples, was ±0.1‰ (1 standard deviation). TOC was analysed both with EA-IRMS and with a LECO-CS230 analyser after removal of carbonate with 4 M HCl. The two methods provided comparable results.

The organic carbon isotope compositions ($\delta^{13}C_{TOC}$) and total organic carbon (TOC_{cf}) contents were measured on 16 samples

from Kelimyar River S5-D1 at the Laboratory of Geology of Lyon: Earth, Planets and Environment (LGLTPE, France). About 0.3–0.4 g of bulk rock powder was decarbonated using 1 M hydrochloric acid for 15 min at ambient temperature. The samples were sequentially rinsed four times with deionized water, with 40 min between rinses to allow the samples to settle before being dried in an oven at 50°C. Between 0.5 and 1 mg of decarbonated powder was weighed into tin capsules and placed in a Pyrocube® elemental analyser connected to an Elementar Isoprime® isotope-ratio mass spectrometer in continuous flow. Each analytical run contained four sets of two standards (IAEA CH7 and caseine) to monitor analytical precision and accuracy. Some samples were replicated and the stable isotope results are reported relative to the 'Vienna Pee Dee belemnite' (VPDB). The precision was better than 0.15‰ for carbon isotope ratio, and 5% of the reported value for TOC contents of the carbonate-free fraction.

4. Results

4.a. Chemostratigraphy

Pliensbachian and Toarcian organic carbon isotope records have been widely used for correlating sections. Although not without caveats related to changes in organic matter composition, as outlined in Suan *et al.* (2015) and van de Schootbrugge *et al.* (2008),
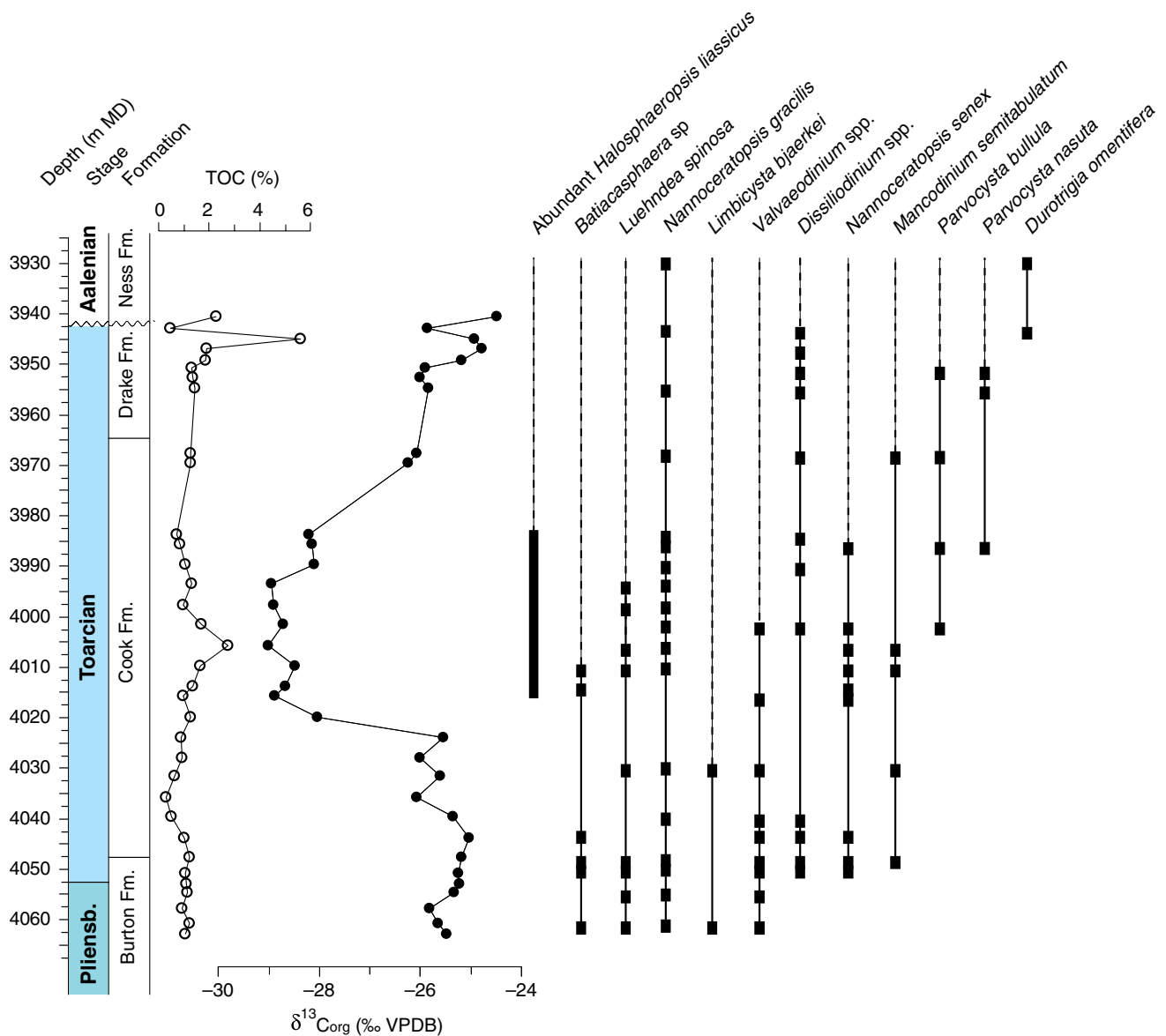
Fig. 6. Range chart and carbon isotope record for the Gulfaks 34/10-35 core.

organic carbon isotope records provide evidence for a prominent negative CIE that has been observed in Toarcian sections around the world (Hesselbo *et al.* 2000, 2007; Hesselbo & Pienkowski, 2011). The negative CIE in the Exaratum Subzone is preceded by a smaller negative excursion at the Pliensbachian–Toarcian boundary that is recorded in only a few locations, most likely because of stratigraphic gaps in many records at this level. In the Siberian and Viking Corridor records this Pliensbachian–Toarcian boundary excursion is missing as a result of erosion and condensation (Figs 3, 5). It is most clearly expressed in the Cleveland Basin record as previously reported by Littler *et al.* (2010; see also Fig. 4). The main negative CIE that marks the T- OAE is recorded in all four bulk organic carbon records presented here. As discussed in Suan *et al.* (2011), the early Toarcian negative CIE occurs in the basal part of the Kurung Member in Siberia (Fig. 3). It constitutes a negative shift of 4–5‰ from an upper Pliensbachian baseline of −26‰. Both sections

show an abrupt shift that indicates erosion of the lowermost Toarcian. Purely based on lithological thickness, the uppermost Pliensbachian is thinner in the KR-S5-D1 section, whereas the base of the Falciferum Zone, corresponding to the onset of organic-rich sedimentation and anoxia, is more expanded. In both sections, the isotope record does not return to pre-CIE or more positive values, which is likely an artefact of organic matter sourcing.

The Gullfaks 34/10-35 core record shows a clear negative CIE starting at 4025 m MD with values decreasing from −26 to −29‰ (Fig. 5). The CIE spans a broad interval and values remain low at *c.* −29‰ until 3985 m MD. Values thereafter increase and reach −24‰ at the erosional contact between the Drake Formation and the Ness Formation. The negative CIE in the Yorkshire record has been well studied, and the record presented here reproduces these older datasets in every detail. Values remain rather low at *c.* −28‰ for much of the Falciferum and Bifrons zones. A modest positive trend of +2‰ is observed for the upper Toarcian Stage.

4.b. Palynostratigraphy

4.b.1. Cleveland Basin

Dinoflagellate cysts are absent from the upper Pliensbachian Staithes Sandstone and base of the Cleveland Ironstone Formation (Fig. 4). This is ascribed to the paralic depositional nature of the succession. The first dinoflagellate cyst species to appear at the top of the Margaritatus Zone is the marker species *Luehndea spinosa*, which is widespread in NW Europe and Tethyan sections and straddles the Pliensbachian–Toarcian boundary. Its extinction has been used to mark the onset of the T-OAE in Tethyan sections (Bucefalo Palliani & Riding, 1999; Bucefalo Palliani *et al.* 2002). The appearance of *L. spinosa* is followed by a veritable regional increase in diversity during the Spinatum Zone with the appearance of key taxa representing several of the characteristic Early Jurassic dinoflagellate lineages, including *Nannoceratopsis deflandrei* subsp. *senex*, *N. deflandrei* subsp. *gracilis*, *Scriniocassis weberi*, *Maturodinium inornatum* and *Valvaeodinium armatum*. The Pliensbachian–Toarcian boundary shows the first appearance of further key taxa, including *Mancodinium semitabulatum* and *Limbicysta bjaerkei*. The lower Toarcian Tenuicostatum Zone witnessed the sustained presence of all these taxa as well as the first appearance of *Wallodinium cylindricum*. The lower part of the Falciferum Zone, coincident with the negative CIE, shows a strong increase in the abundance of amorphous organic matter. The dominant palynomorphs here are *Halosphaeropsis liassica*, small leiospheres most likely representing early maturation stages in the life cycle of prasinophyte green algae (van de Schootbrugge *et al.* 2013). The base of the Mulgrave Shale Member, showing the negative CIE (Exaratum Subzone), is characterized by a marked decrease in dinoflagellate cyst abundance and diversity. All encountered taxa, except for *Wallodinium cylindricum* and *Nannoceratopsis triceras*, range through and reappear after the interval with the negative CIE. However, both *W. cylindricum* and *N. triceras* are extremely rare in the section, which could account for their disappearance.

The transition from the Falciferum to the Bifrons Zone witnessed a further increase in diversity with the first appearance of members of the *Parvocysta–Phallocysta* suite. The first true member of the Parvocystaceae to appear is *Parvocysta bullula*. The boundary between the Falciferum and Bifrons zones also coincides with a lithological change from the paper shales of the Mulgrave Shale Member to the less organic-rich Alum Shale Member. The abundance of *Halosphaeropsis* also decreases across this boundary. In the middle part of the Bifrons Zone the diagnostic species *Susadinium scrofoides* and *Phallocysta eumekes* have their first occurrence (FO). At the boundary between the lower and upper Toarcian Stage, *Scriniocassis priscum* joins some of the longer-ranging taxa such *Mancodinium semitabulatum* and *Nannoceratopsis gracilis*.

Our data are complementary to previous work by Riding (1984) on the Blea Wyke area around Ravenscar (Yorkshire, UK) and by Bucefalo Palliani & Riding (2000) on coastal outcrops between Staithes and Robin Hood's Bay. The study by Bucefalo Palliani & Riding (2000) was mainly directed at the Sinemurian and upper Pliensbachian stages with few samples from the Toarcian Whitby Mudstone Formation. Riding (1984) focused mostly on the upper Toarcian Variabilis to Aalenian Opalinum zones, recognizing many of the same taxa as presented here. Based on all three studies, the following stratigraphic ranges can be precisely delineated. In the Cleveland Basin, the first species of *Nannoceratopsis* and *Mancodinium semitabulatum* appear in the lower Pliensbachian (Ibex Zone) succession, ranging all the way to the base of the

Aalenian Stage. The dinoflagellate cyst assemblages observed from the lower Toarcian Stage are dominated by *Valvaeodinium* and *Nannoceratopsis* with sparse *Mendicodinium*, *Mancodinium* and *Luehndea*. *Scriniocassis weberi* has a continuous range from the Spinatum Zone to the lower Aalenian strata based on the combined records from Riding (1984) and this study. *Phallocysta eumekes* ranges from the middle Bifrons Zone to the Thouarsense Zone. The range of *Scriniocassis priscum* is slightly more extensive based on the work by Riding (1984), occurring as early as in the Bifrons Zone.

The first specimens of *Parvocysta* in the record presented by Riding (1984) occur within the upper Toarcian Variabilis Zone with the first occurrence of *Parvocysta nasuta*, which is slightly above the first occurrence of *P. bullula* noted in this study. *Facetodinium inflatum*, not recognized in this study, first occurs within the upper Toarcian Thouarsense Zone in the study by Riding (1984). *Limbicysta bjaerkei*, recognized by Riding (1984) as *Parvocysta* cf. *barbata*, has a continuous range from the upper Pliensbachian to the Aalenian successions. *Wallodinium cylindricum* has a range from the lower Toarcian Tenuicostatum to upper Toarcian Levesqui Zone, but disappears for most of the middle Toarcian Stage. Finally, Riding (1984) encountered *Escharisphaeridia* sp. in many upper Toarcian samples starting in the Variabilis Zone. Similar specimens were also encountered by us, but they were difficult to quantify. More detailed analyses with regards to this clade are ongoing. This genus shows typical gonyalaucoid paratabulation and archeopyle styles and can be seen as an early representative of the Gonyalaucales, a major Mesozoic lineage of dinoflagellates that rose to prominence during the Bajocian (Wiggan *et al.* 2018).

4.b.2. Gullfaks South Field core 34/10-35

Palynological assemblages for Core 34/10-35 for the upper Pliensbachian Stage from the Burton Formation and Toarcian Drake and Cook formations (Fig. 5) are similar to those from Yorkshire, but differ in several important details. The ranges of *Nannoceratopsis gracilis* and *Mancodinium semitabulatum* are in accordance with many other records from NW Europe. The key species *Luehndea spinosa* ranges across the Pliensbachian–Toarcian boundary and disappears at the height of the negative CIE within the Cook Formation. The range of *Valvaeodinium* is comparable to *L. spinosa*; there is therefore no apparent 'dinoflagellate cyst black-out'. Another striking difference with the Cleveland Basin record is the early inception of gonyalaucoid cysts attributable to the genera *Batiacasphaera* and *Dissiliodinium*. Both cyst types occur in the Pliensbachian succession and range through the interval that contains the negative CIE. Their presence prior to the negative CIE within the Viking Corridor suggests a much earlier inception of these gonyalaucoid cysts when compared with the British records. Third, and perhaps most important, is the first inception of members of the *Parvocysta*-suite coincident with the negative CIE. *Parvocysta bullula* and *P. nasuta* have their first appearances within the middle part of the Cook Formation, which, based on the C-isotope stratigraphy, is equivalent to the lower Toarcian Stage.

4.b.3. Kelimyar River S16

The Kelimyar River (KR) Section S16 shows distinct palynological assemblages for Pliensbachian and Toarcian formations (Figs 7, 8). Within the KR-S16 section, the lower part of the upper Pliensbachian Kyra Formation (Viligaensis Zone) is characterized by abundant terrestrial organic matter. Dinoflagellate cysts in this
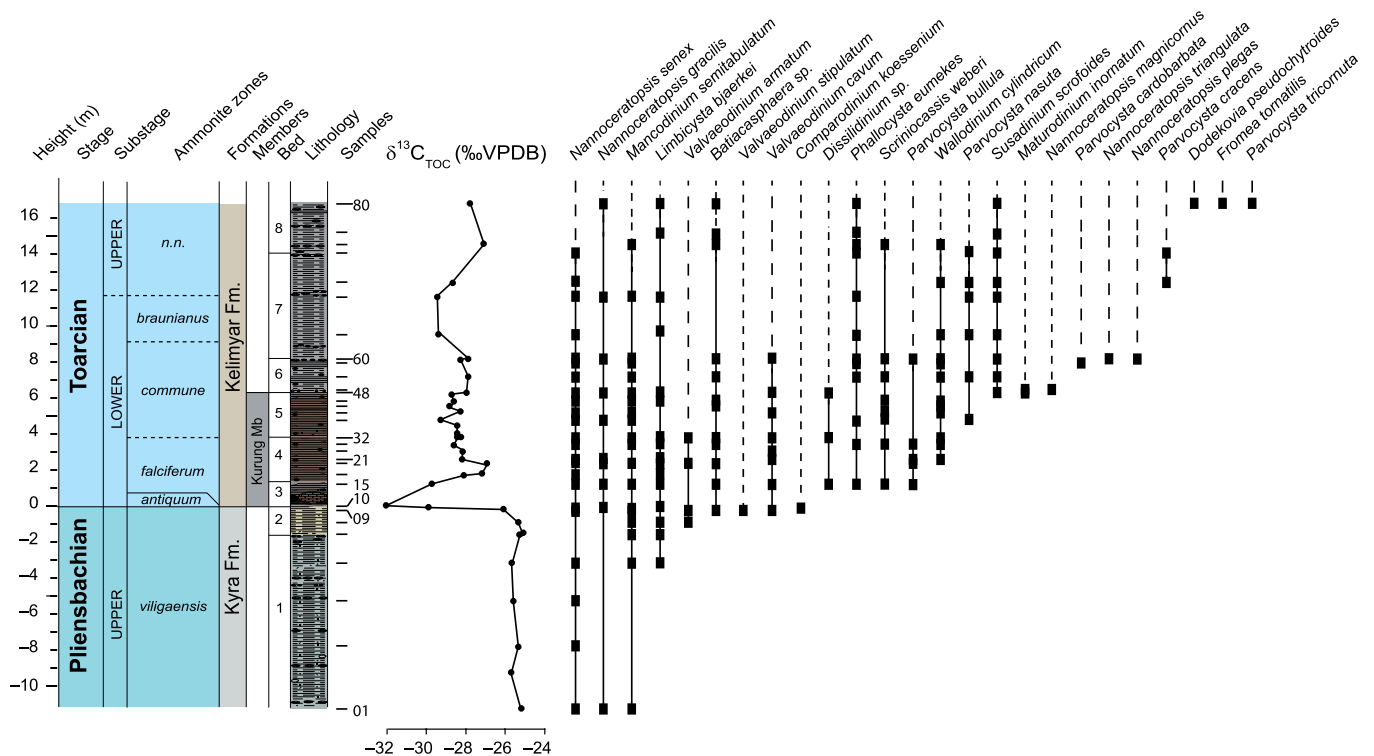
Fig. 7. Range chart for the Kelimyar River S16 section showing selected dinoflagellate species. A number of dinoflagellate cysts are undescribed and not included in the chart.

interval are sparse and dominated by *Nannoceratopsis senex* and *N. gracilis* and rare *Mancodinium semitabulatum*. Other marine elements include rare prasinophyte phycomata and acritarchs. The uppermost part of the Kyra Formation shows a clear increase in marine influence with the appearance of *Limbicysta bjaerkei*, and especially in sample KR-S16(09) where *Valvaeodinium armatum*, *V. stipulatum*, *V. cavum* and *Batiacasphaera sp.* have their first appearances.

The transition to the lower Toarcian Kurung Member of the Toarcian Kelimyar Formation shows a dramatic increase in the amount of marine palynomorphs with abundant remains of acritarchs, dinoflagellate cysts and prasinophytes. The lowermost Toarcian Antiquum Zone is highly condensed and only represented by sample KR-S16(10). However, this sample shows a clear increase in dinoflagellate diversity. *Nannoceratopsis deflandrei* subsp. *senex*, *Mancodinium semitabulatum* and *Limbicysta bjaerkei* continue to be present. A number of genera and species have a first occurrence in this sample (see Fig. 5), including *Valvaeodinium stipulatum*, *Comparodinium punctatum*, *Valvaeodinium armatum* and *Batiacasphaera* sp. Members of the *Parvocysta–Phallocysta* suite might be present, but the preservation is not good enough in this sample to be absolutely sure and their identification has to await further analysis. Sample KR-S16(10) shows a brief decline in diversity, but many of the species (*M. semitabulatum*, *N. senex* and *M. inornatum*) that were present below continue within this sample and beyond. Sample KR-S16(12) is the only sample in this set of 33 samples that is devoid of any structured palynomorphs, which is likely a taphonomic problem. Curiously enough, this sample, with the most negative C-isotope value within the Toarcian negative CIE, is entirely dominated by phytoclasts.

Sample KR-S16(15) coincides with the returning limb of the negative CIE within the Falciferum Zone. This sample shows a marked increase in diversity. Many of the species present prior

to the negative CIE continue. In addition, this sample marks the first appearance of *Scriniocassis weberi*, *Phallocysta eumekes*, *Parvocysta bullula* and dinoflagellate cysts attributable to the genus *Dissiliodinium*. Afterwards, diversity continues to increase gradually up until the top of the Commune Zone (sample KR-S16(60)) with the addition of *Susadinium scrofoides*, *Wallodinium cylindricum*, *Parvocysta nasuta* and *Maturodinium inornatum*. In this interval we also observed several species of *Nannoceratopsis deflandrei* subsp. *senex* other than *N. senex* and *N. gracilis*, including *N. triangulata*, *N. plegas* and *N. magnicornus*. Diversity decreases again in the Braunianus Zone, which is likely an artefact of changes in lithology and decreased preservation. *Parvocysta cracens* occurs briefly around the lower–upper Toarcian boundary, and perhaps this species is a good marker for this boundary in high-latitude settings. The uppermost sample, KR-S16(80) from the upper Toarcian Stage, shows the appearance of several additional species, including *Fromea tornatilis* and *Dodekovia pseudochytroides*, as well as *Parvocysta tricornuta*. Although *Fromea tornatilis* is not generally accepted as a dinoflagellate cyst, the first two species were previously only known from the Aalenian–Bajocian stages of NW Europe; the latter occurs in the upper Toarcian Hebrides Basin (Scotland; Riding *et al.* 1991). Overall, the Kelimyar River S16 record does show the much earlier inception of the *Parvocysta–Phallocysta* suite, with many key species appearing during the early Toarcian Age.

4.b.4. Kelimyar River S5-D1

Although very much condensed, this section is extremely important for examining the inception of the *Parvocysta–Phallocysta* suite during the early Toarcian Age. The 10 samples investigated are from the very top part of the Kyra Formation (sample KR-S5-D1(05)) and the lowermost 1.5 m of the Kelimyar Formation (Kurung Member) that shows the negative CIE (Fig. 9). Sample S5(05) shows moderately abundant *Valveaeodinium stipulatum*
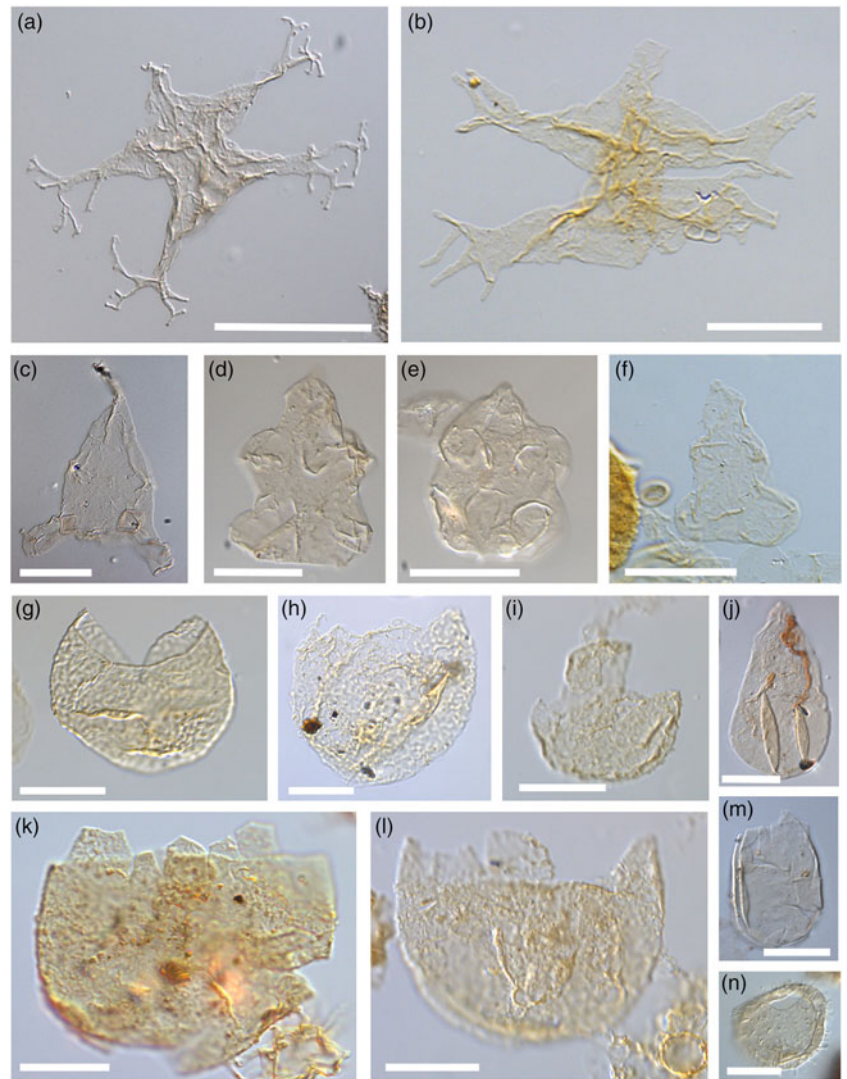
Fig. 8. Selected Pliensbachian and Toarcian dinoflagellate cyst species from Kelimyar River section S16 (all scale bars, 20 μm). (a) *Limbicysta bjaerkei*: sample S16-07 from the Viligaensis Zone, upper Pliensbachian. Note the extremely bifurcated processes, illustrating intraspecific variability. (b) *Limbicysta bjaerkei*: sample S16-80 (Kelimyar Formation), upper Toarcian. Note the generally more robust shape and processes compared with the Pliensbachian specimen. (c) *Parvocysta cracens*: sample S16-71 from the upper Toarcian Kelimyar Formation. (d) *Susadinium scrofoides*: sample S16-48 from the Commune Zone (lower Toarcian, Kelimyar Formation). (e) *Parvocysta bullula*: sample S16-60 from the Commune Zone (lower Toarcian, Kelimyar Formation). (f) *Parvocysta tricornuta*: sample S16-80 from the upper Toarcian (Kelimyar Formation). (g) *Batiacasphaera* sp. A: sample S16-80 from the upper Toarcian (Kelimyar Formation). (h) *Batiacasphaera* sp. B: sample S16-27 from the Falciferum Zone (lower Toarcian, Kelimyar Formation). (i) *Dissiliodinium* sp.: sample S16-30 from the Falciferum Zone (lower Toarcian, Kelimyar Formation). (j) *Phallocysta eumekes*: sample S16-60 from the Commune Zone (lower Toarcian, Kelimyar River). (k) *Mancodinium semitabulatum*: sample S16-09 from the Viligaensis Zone (Kyra Formation, upper Pliensbachian) (l) *Mancodinium semitabulatum*: sample S16-30 from the Falciferum Zone (lower Toarcian, Kelimyar Formation). (m) *Valvaeodinium aquilonium*: sample S16-49 from the Commune Zone (lower Toarcian, Kelimyar Formation). (n) *Valvaeodinium cavum*: sample S16-21 from the Falciferum Zone (lower Toarcian, Kelimyar River).

in addition to other more poorly preserved specimens of *Valvaeodinium* sp. With the onset of the Toarcian negative CIE, we observe a dramatic rise in species diversity with the first appearance datums (FADs) of *Valvaeodinium aquilonium*, *Susadinium scrofoides*, *Wallodinium laganum*, *Dodekovia pseudochytroides*, *Batiacasphaera* sp., *Phallocysta elongata* and *Mancodinium semitabulatum* (see also Fig. 10). At the top of the black shale at the base of the Kurung Member more species appear, including *Fromea tornatilis*, *Moesiodinium raileanui*, *Phallocysta eumekes* and *Parvocysta bullula*. Sample KR-S5-D1(11) contains several species of *Parvocysta*, including *P. contracta*, *P. nasuta* and *Facetodinium inflatum*. Surprisingly, *Nannoceratopsis* species are largely missing, except for higher up in samples KR-S5-D1(14) to (18). These latter samples contain less dinoflagellate cysts, but instead contain abundant amorphous organic matter.

Sections in the Arctic part of the Eastern Siberia Basin, especially in the Anabar and Olenek river deltas, have been investigated previously for palynology and palynostratigraphy by various Russian workers. An enormous body of work was compiled, summarized and complemented by additional analyses in Riding *et al.* (1999). However, analysis of outcrops along the Kelimyar River was only represented by a single sample (NS53; Riding *et al.* 1999) from the lowermost upper

Toarcian strata. That sample was overwhelmingly dominated by several species of *Nannoceratopsis* and *Phallocysta eumekes*, in addition to rare *Parvocysta cracens*, *Susadinium scrofoides* and *Valvaeodinium aquilonium* (Riding *et al.* 1999). A higher-resolution study was carried out on sections along the Anabar River spanning the upper Pliensbachian to lower Toarcian successions (two sections, approximately 40 samples; Riding *et al.* 1999). In those sections, the upper Pliensbachian Viligaensis Zone produced sparse assemblages dominated by *Nannoceratopsis deflandrei* subsp. *anabarensis* and *N. deflandrei* subsp. *senex*. These two subspecies of *N. deflandrei* also dominate the lower Toarcian Propinquum (=Antiquum), Falciferum and Commune zones. In addition, Riding *et al.* (1999) mention *Mancodinium semitabulatum* and *N. gracilis* as dominant taxa in the lower Toarcian Stage. All common members of the *Phallocysta*–*Parvocysta* suite are consistently observed in the upper Toarcian strata by Riding *et al.* (1999). Species of *Valvaeodinium*, which are already clearly present within the uppermost Pliensbachian and lowermost Toarcian stages, were only observed within the upper Toarcian Stage in the compilation presented by Riding *et al.* (1999). The study by Goryacheva (2017), who worked essentially on the same sample set from sections KR-S16 and KR-S5-D1, produced slightly different results from those presented in Riding *et al.* (1999). Most notably,
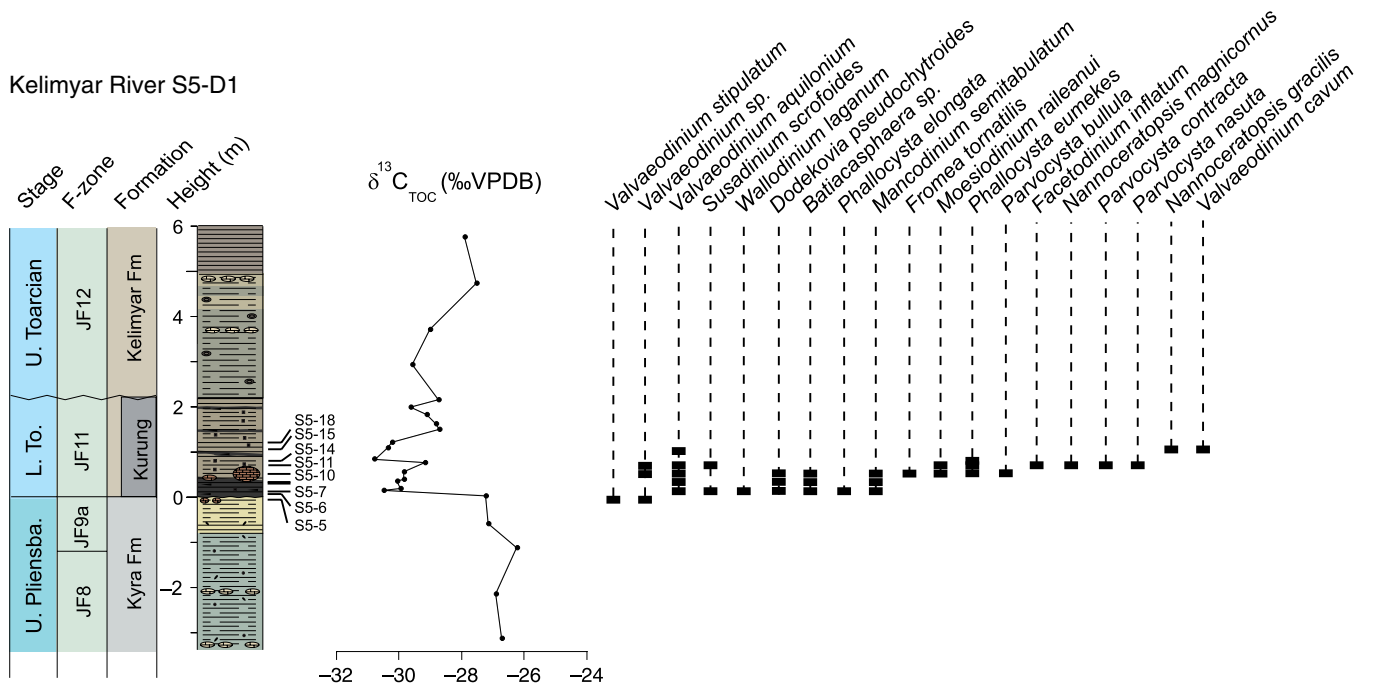
Kelimyar River S5-D1

Fig. 9. Range chart for Kelimyar River section S5-D1 with selected dinoflagellate species. A number of species are undescribed and not included in this chart.
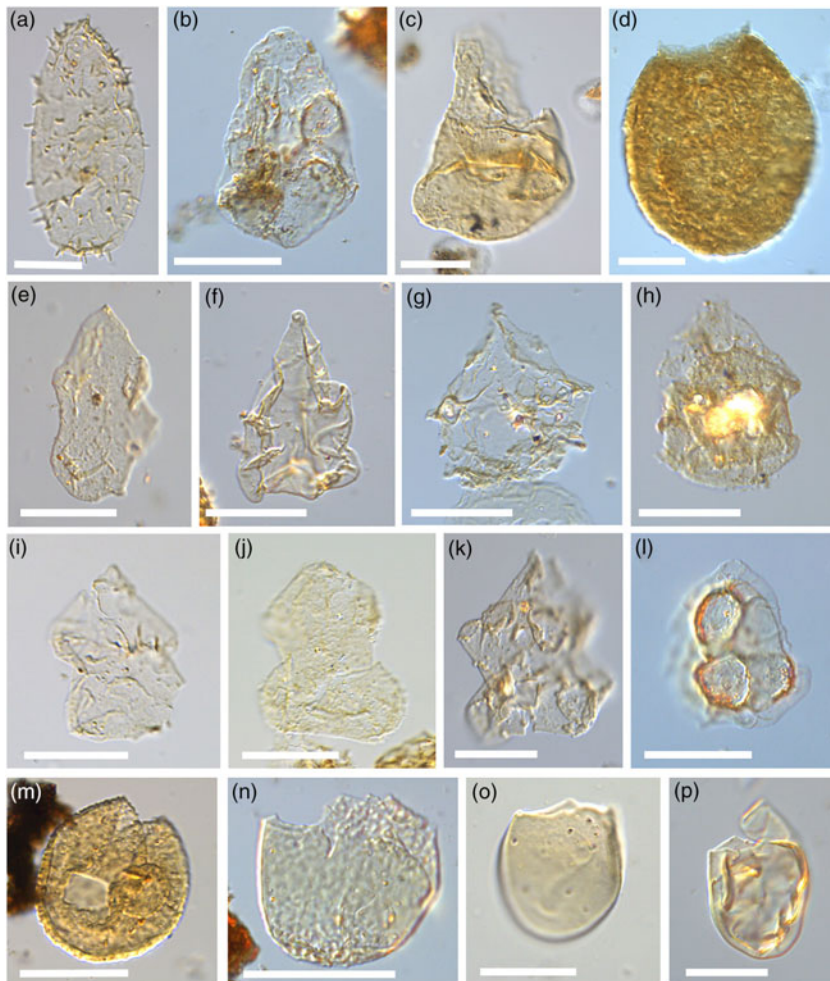

Fig. 10. Selected Pliensbachian and Toarcian dinoflagellate cyst species from Kelimyar River section S5-D1 (all scale bars, 20 μm). (a) *Valvaeodinium stipulatum*: sample S5-05 from the upper Pliensbachian (Kyra Formation). (b) *Phallocysta elongate*: sample S5-07 from the base of the Kurung Member (lower Toarcian). (c) *Phallocysta eumekes*: sample S5-10 from the base of the Kurung Member (lower Toarcian). (d) *Fromea tornatilis*: sample S5-10 from the base of the Kurung Member (lower Toarcian). (e) *Facetodinium inflatum*: sample S5-09 from the base of the Kurung Member (lower Toarcian). (f) *Parvocysta bullula*: sample S5-09 from the base of the Kurung Member (lower Toarcian). (g) *Parvocysta nasuta*: sample S5-11 from the Kurung Member (lower Toarcian). (h) *Moesiodinium raileanui*: sample S5-10 from the base of the Kurung Member (lower Toarcian). (i) *Parvocysta nasuta*: sample S5-11 from the Kurung Member (lower Toarcian). (j) *Parvocysta contracta*: sample S5-11 from the Kurung Member (lower Toarcian). (k) *Susadinium scrofoides*: sample S5-11 from the Kurung Member (lower Toarcian). (l) *Moesiodinium raileanui*: sample S5-07 from the base of the Kurung Member (lower Toarcian). (m) *Dodekovia pseudochytroides*: sample S5-07 from the base of the Kurung Member (lower Toarcian). (n) *Batiacasphaera* sp. A: sample S5-07 from the base of the Kurung Member (lower Toarcian). (o) *Valvaeodinium aquilonium*: sample S5-07 from the base of the Kurung Member (lower Toarcian). (p) *Wallodinium laganum*: sample S5-07 from the base of the Kurung Member (lower Toarcian).

Goryacheva ([2017](#)) documents the presence of *Phallocysta eumekes* and several other "typical" upper Toarcian NW European species, such as *Fromea*, already in the lower Toarcian Kurung Member.

The striking differences between the records from Siberia presented by Riding *et al.* ([1999](#)) and Goryacheva ([2017](#)), and between these records and those presented here, could be due to a number of reasons. Although the study by Riding *et al.* ([1999](#)) was generally of lower resolution, the authors did look at a much greater number of sections, so we would expect them to find a similar overall diversity. Taphonomy and regional palaeo-environmental settings could also be issues as most dinoflagellate cysts are extremely thin-walled and preservation, especially in intervals rich in amorphous organic matter, is poorer. Sample location could also be an issue; our study suggests that KR-S5-D1 contains a higher diversity than section KR-S16. The two sections are more than 60 km apart, so the possibility of regional differences in palaeodepths is plausible. The KR-S16 section shows a predominance of *Nannoceratopsis* species, which seem to be mostly absent from the KR-S5-D1 section. Other striking differences include the abundance and continued presence within the Toarcian Stage of specimens grouped under *Batiacasphaera* in the KR-S16 section and the diverse and abundant presence of members of the *Parvocysta*-suite in the lowermost Toarcian strata in the KR-S5-D1 section. These are likely due to regional differences in bathymetry. As the study by Goryacheva ([2017](#)) was carried out on the same sample set, it seems that different methods of preparation of samples could be an issue. Goryacheva ([2017](#)) mentions the use of heavy liquid to separate minerals from palynomorphs; this technique can lead to loss of small palynomorphs that have pyrite infilling.

5. Discussion

5.a. High-latitude dinoflagellate diversity

The high latitudes have played a pivotal role in understanding the evolution of cyst-producing dinoflagellates (Riding & Ioannides, [1996](#); Mangerud *et al.* [2019](#)). Sections in Arctic Canada have yielded some of the oldest and also most diverse dinoflagellate cyst assemblages dating back to the Late Triassic Period (Wiggins, [1973](#), [1978](#); Bujak & Fisher, [1976](#)). Work on phosphorite nodules from the Toarcian Brentskardhaugen Bed on Spitsbergen produced the earliest evidence for the previously unknown *Parvocysta* suite (Bjaerke, [1980](#)). Work by Davies ([1983](#)) on a dinoflagellate cyst zonation for the Sverdrup Basin of Arctic Canada showed the presence of a diverse algal community with at least 18 Toarcian species. Prauss ([1989](#)) speculated that early dinoflagellate cyst diversity was higher in the northern high latitudes as many species tend to have earlier first occurrences there when compared with low latitudes. A northern high-latitude origin for the *Parvocysta–Phallocysta* suite was suggested by Feist-Burkhardt & Wille ([1992](#)) and Riding & Ioannides ([1996](#)) based on palynological records from southern Germany and the UK, respectively. However, precise evidence for the high-latitude origin of the *Parvocysta–Phallocysta* suite has been generally lacking because of a dearth in studies on systematically sampled sections.

Abundant and diverse lower Toarcian Falciferum Zone dinoflagellate cyst assemblages in the Kelimyar River sections are both interesting and at odds with records of similar age from NW Europe and the Mediterranean area, such as in Germany, the UK and the Lusitanian Basin (Portugal). For example, in Portugal only two genera (*Nannoceratopsis* and *Mancodinium*) are present across the T-OAE (Correia *et al.* [2017](#)), which is unlikely solely related

to taphonomic issues. Further, the *Phallocysta–Parvocysta* suite is entirely missing from many Tethyan sections (Davies, [1985](#); Poulsen & Riding, [2003](#); Riding & Ioannides, [1996](#)). Across NW Europe, organic-matter-rich shales of early Toarcian age are characterized by low-diversity dinoflagellate cyst assemblages; in particular, sections that contain extensive laminated black shales (Posidonia shales) are normally devoid of dinoflagellate cysts. In southern Germany, the Unterer and Oberer Schiefer (Lias Epsilon), equivalent to the Falciferum Zone, only contain *Nannoceratopsis deflandrei* subsp. *gracilis*, *Comparodinium punctatum* and *C. lineatum* (Wille, [1982](#)).

Palynological studies carried out in Italy, Germany and the UK provide strong evidence for a rapid spread of the *Parvocysta–Phallocysta* suite across Europe during late Toarcian time. In Germany, Wille ([1982](#)) described *Parvocysta nasuta* from the Fibulatum Subzone (Bifrons Zone). In his very extensive monograph on dinoflagellate taxonomy and diversity from northern Germany, Prauss ([1989](#)) documented in great detail the late Toarcian diversification of the *Parvocysta–Phallocysta* suite. In a review of dinoflagellate cyst biostratigraphy for the Danish Sub-basin, Poulsen ([1992](#)) introduced a "Parvocysta Subzone" based on the first and last occurrences of a whole suite of *Parvocysta* species, including *P. barbata*, *P. bjaerkei* (=*Limbicysta bjaerkei*), *P. bullula*, *P. cracens*, *P. nasuta*, *Susadinium faustum* and *S. scrofoides*. The age of this subzone is early middle Toarcian (Bifrons Zone) to Aalenian. Work by Bucefalo Palliani *et al.* ([1998](#)) on the upper Toarcian – Aalenian Wittnau core from Germany showed a maximum diversity for the *Parvocysta* group within the uppermost Toarcian strata. Feist-Burkhardt & Pross ([2010](#)) also showed high abundances and diversity of the *Parvocysta–Phallocysta* suite in the uppermost Toarcian and basal Aalenian successions in the Hausen core from southern Germany. Whereas records from South America tend to lack independent age control, the first members of the *Parvocysta–Phallocysta* suite appear in the uppermost Toarcian Neuquen Basin in Argentina (Zavattieri *et al.* [2008](#)), which could be taken as evidence for a progressive migration from northern high latitudes to southern low latitudes during the course of the Toarcian Age.

The early Toarcian disappearance of dinoflagellate cysts following a late Pliensbachian radiation has been described as a "dinoflagellate cyst black-out" and is widely seen as a result of the inimical conditions within the water column coinciding with the Toarcian Oceanic Anoxic Event (Bucefalo Palliani *et al.* [1998](#)). Indeed, one of the most common and abundant late Pliensbachian – earliest Toarcian species, *Luehndea spinosa*, appears to have gone extinct across northern Europe with the onset of black shale deposition (Bucefalo Palliani & Riding, [1999](#)). The Siberian and Viking Corridor records paint a completely different picture, with numerous dinoflagellate species present at the height of the Toarcian OAE. Instead of being a "dinoflagellate cyst black-out", the Toarcian OAE interval in northern high latitudes was an interval of rapid diversification with high diversity and abundance. Moreover, early inceptions of the *Parvocysta–Phallocysta* suite in Siberia were accompanied by the early appearance of members of the Gonyaulacales, including many undescribed specimens assigned to *Escharisphaeridia*, *Batiacasphaera* and *Dissiliodinium*. These genera typically appear during latest Toarcian – Aalenian time, while several other genera such as *Fromea* are characteristic of the Aalenian–Bajocian interval. From this, we conclude that the high northern latitudes likely functioned as a cradle for dinoflagellate evolution. The enormous diversity recorded in the KR-S5-D1 section also suggests that this evolution was ongoing.

To determine whether it was triggered by carbon injection and enhanced greenhouse warming needs further work, but it could prove to be a pivotal example of the link between greenhouse warming and changes in ecosystem structure and evolution in high-latitude settings.

5.b. Arctic connectivity and circulation through the Viking Corridor

The presence of a diverse lower Toarcian (Falciferum Zone) assemblage of cyst-producing dinoflagellates in Siberia and the Viking Corridor, particularly the presence of the *Parvocysta–Phallocysta* suite, has implications for our understanding of Early Jurassic oceanography. The sudden inception of the *Parvocysta–Phallocysta* suite in NW Europe during the late early Toarcian Age (Bifrons Zone) and its further diversification during the late Toarcian Age indicates that an important connection existed between the Arctic Sea and the Tethys Ocean, allowing these phytoplankton taxa to migrate southwards. Our data strongly point towards the establishment of a S-directed circulation through the Viking Corridor at the Falciferum–Bifrons transition. Since some homogenization of dinoflagellate communities occurred prior to the Toarcian OAE during the late Pliensbachian Age, with both the Arctic and Tethys regions showing communities dominated by members of Valvaeodiniaceae and Nannoceratopsiaceae and the cosmopolitan *Mancodinium*, passages were likely open during the entire Pliensbachian–Toarcian interval.

The delayed arrival of the *Parvocysta–Phallocysta* suite in NW European basins during the Bifrons Zone relative to the spread of *Nannoceratopsis* and *Valvaeodinium* species suggests that some physical or chemical barrier existed that inhibited the *Parvocysta–Phallocysta* suite to migrate southwards. The widespread genus *Nannoceratopsis* was likely adapted to coastal habitats and low-salinity, perhaps even brackish, waters. In contrast, *Parvocysta–Phallocysta* taxa that dominate the lower Toarcian Stage in Siberia are considered here to have been open-marine taxa. Hence, the arrival of the *Parvocysta–Phallocysta* suite in NW Europe was either driven by eustatic sea-level rise or by tectonic subsidence in the Viking Corridor allowing taxa to spread through the gateway. Indeed, sea-level reconstructions for NW Europe indicate a lowstand during earliest Toarcian time and highstands for the Falciferum–Bifrons transition. In Germany, this level is marked by the Monotis Beds or "Inoceramenbank", strongly condensed beds rich in bivalves marking a maximum flooding surface (Röhl *et al.* 2001; Rohl & Schmid-Röhl, 2005).

Surface water connection through the Viking Corridor played a crucial role in determining oxygenation of basins at the southern end of the strait across the EES as suggested and reviewed extensively by Korte *et al.* (2015). This flow was likely controlled by tectonic movements modulated by changes in eustatic sea level and perhaps autocyclic infilling. Sedimentary successions within the Viking Corridor are a key piece of the puzzle and inform us of water depth in the corridor. In the Viking Graben area of the northern North Sea (Fig. 2), Lower Jurassic sediments conformably overlie Triassic strata. Upper Triassic – lowermost (Hettangian) Jurassic strata are characterized by the massive deltaic sandstones of the Statfjord Group (Lervik, 2006). The remainder of the Lower Jurassic succession (Sinemurian – base Aalenian) comprises the Dunlin Group, which is divided into (from base to top) the Amundsen, Johansen, Burton, Cook and Drake formations (Vollset & Dore, 1984). The Amundsen and Burton formations represent fine-grained paralic estuarine to proximal marine shelfal mudstones, whereas the Johansen and Cook formations represent coarser-grained sandstone end-members.

The coarse clastic material of the Cook Formation was sourced from the eastern basin margin and prograded westwards (Chamock *et al.* 2001; Husmo *et al.* 2003). Hence, the Cook Formation was deposited at a time when shallow-marine waters had transgressed over parts of the deltaic to paralic Triassic and Lower Jurassic strata (Steel, 1993) and formed a very shallow and narrow seaway, essentially bounded by the Shetland Platform in the west and the Fennoscandian hinterland in the east (Husmo *et al.* 2003). The Cook Formation can be divided into four to five distinct sandy units, with regressive–transgressive segments that can be traced straightforwardly on petrophysical logs (Chamock *et al.* 2001). As a consequence, the upper part of the Dunlin Group is often interpreted in terms of alternations between sandy (Cook Formation) and mudstone (Drake Formation) facies. Above the fourth and uppermost Cook Formation sandstone, the widespread, conspicuous, dark, episodically calcareous Drake Formation claystone unit occurs (Chamock *et al.* 2001). The latter is interpreted to mark progressive deepening of the Viking Corridor. Based on our C-isotope correlations, this deepening occurred during the Bifrons Zone, at the time when Arctic dinoflagellates appeared in NW Europe and when conditions changed from euxinic to anoxic.

Interestingly, the *Parvocysta–Phallocysta* suite disappeared from NW European basins during the Aalenian Age (Prauss, 1989) and their range tops make good stratigraphic markers (Feist-Burkhardt & Pross, 2010). The Aalenian Stage was marked by thermal doming in the North Sea region effectively interrupting southwards flow through the Viking Corridor. Within the Viking Corridor the Brent Group marks the arrival of shallow-marine deltaic deposits that unconformably overly the Cook and Drake formations. Reorganization of circulation in the northern North Sea could explain the cooling that is observed in belemnite oxygen isotope records from the Hebrides Basin in Scotland (Korte *et al.* 2015). The disappearance of the *Parvocysta–Phallocysta* suite may be linked to interruption of flow through the Viking Corridor. Whether these dinoflagellates continued to thrive in high northern latitudes remains to be determined. Understanding their evolutionary trajectories in the Arctic will likely inform us of the cause of their demise.

5.c. Implications for Toarcian palaeoceanographic models

Our new data have clear implications for palaeoceanographic models that have been invoked to explain salinity stratification within the EES leading to the T-OAE. The influx of low-salinity Arctic waters through the Viking Corridor can be ruled out as a driver of stratification and anoxia (Prauss & Riegel, 1989; Prauss *et al.* 1991), since these waters arrived across the transition from the Falciferum to Bifrons zones, well after the onset of anoxia in NW Europe. Our results are fully incompatible with a recently proposed scenario in which melting ice caps that had supposedly developed during the late Pliensbachian Age drove a sea-level rise of 100 m and led to low-salinity water influx at the onset of the T-OAE (Ruebsam *et al.* 2019). Instead, stratification and poor mixing of basins in the EES and along the western Tethys margin can be fully explained by increased run-off from Laurasia under enhanced greenhouse climate conditions, combined with restriction of basins (McArthur *et al.* 2008) due to sea-level changes and circulation in the Tethys Ocean (Ruvalcaba Baroni *et al.* 2018). Enhanced run-off from Laurasia is supported by clay mineral data from across the EES that shows elevated chemical
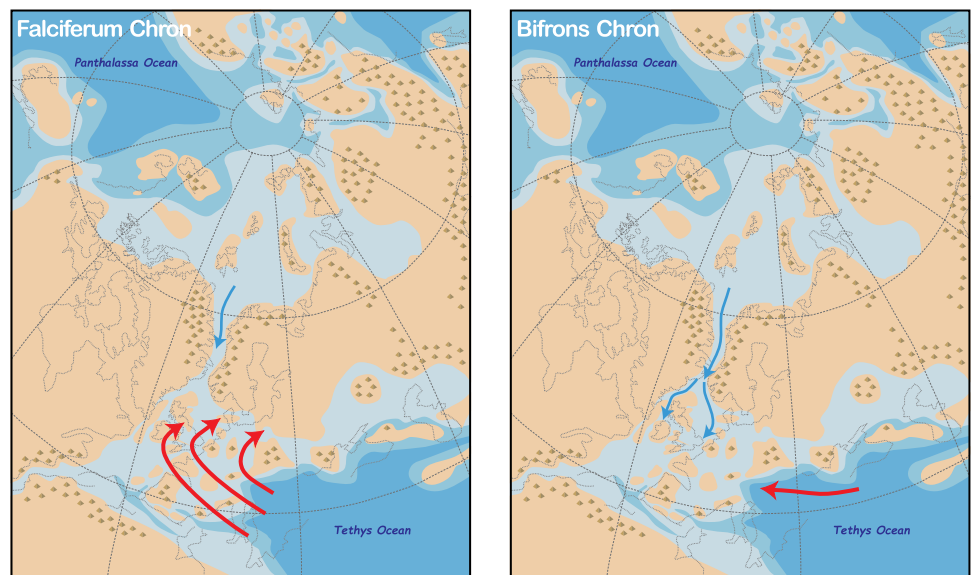
Fig. 11. Circulation through the Viking Corridor during the Falciferum and Bifrons chrons. During the Falciferum Chron, strong clockwise circulation in the Tethys brought warm saline waters onto the shelves that were capped by low-salinity waters from enhanced run-off. During the Bifrons Chron, reduced intensity of circulation in the Tethys and flooding of the Viking Corridor during a general highstand triggered the influx of colder low-salinity water from the Arctic, leading to the rapid spread of the *Parvocysta–Phallocysta* suite in NW Europe.

weathering on the continents (Cohen *et al.* 2004) and the influx of kaolinite (Raucsik & Varga, 2008; Dera *et al.* 2009a), a clay mineral that is widely understood to form under conditions of extreme humidity.

Reconstructions of Jurassic circulation between the Arctic Sea and Tethys Ocean have relied on geochemical proxies, faunal migrations and output from coupled ocean–atmosphere models. Work on ammonite and foraminifera diversity suggests that the Viking Corridor served as a major gateway for faunal exchange between high- and low-latitude communities (Nikitenko & Mickey, 2004; Zakharov *et al.* 2006). Ammonite faunas show signs of maximum separation during the Late Pliensbachian, but faunas became entirely homogenized during the Falciferum Zone with Tethyan ammonite families such as the Dactylioceratinae migrating northward into Arctic basins (Dera *et al.* 2011). Foraminifera, ostracodes and bivalves show a major turnover across the Pliensbachian–Toarcian boundary in Siberia, which has been explained by migration through the Viking Corridor due to changes in sea level and climate (Nikitenko & Shurygin, 1994; Nikitenko & Mickey, 2004; Zakharov *et al.* 2006).

The early Toarcian Age witnessed two large migrations of foraminifers and ostracods to Arctic and western European basins (Nikitenko & Mickey, 2004; Nikitenko, 2008, 2009; Nikitenko *et al.* 2008). The first migration occurred in the earliest Falciferum Chron associated with eustatic sea-level rise and considerable climate warming. Thermophylic microfauna that migrated to the Arctic Sea were not common and did not evolve there. In contrast, Arctic forms that migrated to the low-latitude seas often became successful in marginal environments. A second period of considerable migrations occurred in the Commune Chron (= Bifrons Chron; Fig. 6). Representatives of Arctic microfauna that migrated to western European seas often did establish themselves there. For example, representatives of *Camptocythere* (Ostracoda) appeared at the beginning of the early Toarcian Age (earliest Falciferum Chron) in the Arctic, migrated into western European seas through the Viking Corridor in the first half of the Commune Chron, and further existed there during the late Toarcian – Middle Jurassic interval (Triebel, 1950; Bate & Coleman, 1975; Ainsworth, 1986; Nikitenko & Mickey, 2004; Nikitenko, 2009).

The northwards spread of low-latitude organisms has been interpreted to reflect the generally northwards flow through the Viking Corridor during much of the Early Jurassic Period (Korte *et al.* 2015). However, this is not reflected in geochemical proxy records and coupled ocean–climate models. Nd-isotopes obtained from Early Jurassic fish remains were used to determine the influence of the Viking and Hispanic corridors during the onset of the T-OAE, but diagenetic problems leading to a low-resolution dataset made it difficult to draw very firm conclusions (Dera *et al.* 2009b). However, Dera *et al.* (2009b) did envision a predominantly southwards flow through the Viking Corridor during the Pliensbachian–Toarcian ages with relatively unradiogenic Arctic water entering the Tethys. Oxygen isotope records from belemnite calcite show a pronounced shift towards more negative $\delta^{18}O$ values at the onset of the T-OAE, which has been attributed to a concomitant decrease in salinity and a temperature rise of up to 7°C (Bailey *et al.* 2003). Belemnite oxygen isotope values remain relatively stable after the T-OAE, which Korte *et al.* (2015) interpreted as reflecting stable temperatures in NW Europe. However, these authors ignore the influence of salinity changes on belemnite oxygen isotope values. We suggest that the apparent stability in oxygen isotope values could be driven by a change in salinity, whereby the influx of low-salinity waters masked temperature effects.

Reconstructions of circulation that rely on numerical models (Bjerrum & Surlyk, 2001; Dera & Donnadieu, 2012; Ruvalcaba Baroni *et al.* 2018) have reached remarkably consistent conclusions about the direction of flow through the Viking Corridor. All these models show predominant southwards flow of low-salinity waters from the Arctic into the Tethys. The most up-to-date model presented by Ruvalcaba Baroni *et al.* (2018) indicates that, under high atmospheric pCO_2 conditions such as during the Toarcian Age, oceanographic conditions in the EES were dominated by strong clockwise circulation in the Tethys bringing warm saline waters onto European shelves (Fig. 11). This strong circulation may have diminished the effects of flow through the Viking Corridor, which was further shunted by sedimentation, eustacy and tectonics in the corridor. Lowered pCO_2 following the T-OAE may therefore have led to a decrease in the strength of Tethyan flow and enhanced the influence of Arctic influx. Such a change in dominant flow can be
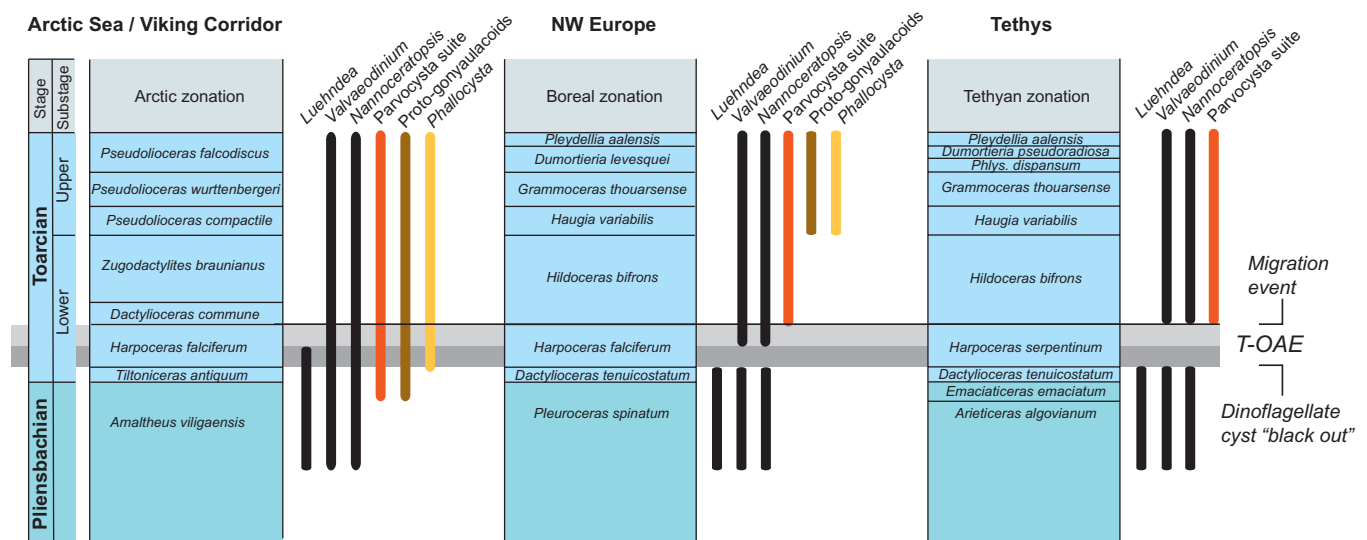
Fig. 12. Range charts for selected genera showing southwards migration of the *Parvocysta–Phallocysta* suite into NW Europe and the Tethys. Phallocysta is absent from southern Europe. Early gonyaulacoid cysts occur within the Arctic and Viking Corridor, but appear only much later in NW Europe. The sudden appearance of the *Parvocysta–Phallocysta* suite coincides with the end of the most intense euxinic conditions across basins in the European Epicontinental Seaway.

compared with a switch from an anti-estuarine circulation with inflowing warm saline waters from the Tethys, capped by low-salinity waters from run-off during the T-OAE, to an estuarine circulation with the influx of colder, nutrient- and oxygen-rich waters from the Arctic during the Bifrons Zone.

5.d. The end of an euxinic event in NW Europe

The transition from the early Toarcian Falciferum to Bifrons Chron was a major turning point in the development of the T-OAE in both the Arctic and the Tethyan realms and is clearly marked in biotic and geochemical proxy records. TOC values decrease across this boundary to more modest levels from their absolute highest values within the Exaratum Zone. Carbon isotope records show a positive excursion at this level that is generally masked in organic carbon isotope records by organic matter composition, but clearly shows up in many carbonate carbon isotope records (Suan *et al.* 2015). The enrichment of redox-sensitive elements has been widely used to reconstruct oxygenation and restriction of basins across the T-OAE (McArthur *et al.* 2008). Mo and As show enrichment during the Falciferum Zone in Yorkshire, but values show a strong decline across the Falciferum–Bifrons transition (Thibault *et al.* 2018). Total sulphur and degree of pyritization show similar trends (Thibault *et al.* 2018).

Carbonate-associated sulphur isotope ($\delta^{34}S_{cas}$) records obtained from belemnite calcite show a positive excursion within the upper part of the Falciferum Zone that has been correlated with the positive excursion in carbon isotope records (Gill *et al.* 2011). Rather than declining to background values as organic matter burial and presumably associated pyrite burial dwindled, the $\delta^{34}S_{cas}$ isotope values remain generally very high from this point onwards in the UK and Germany for the duration of the Toarcian Age (Gill *et al.* 2011; Newton *et al.* 2011). The high values in $\delta^{34}S_{cas}$ for the upper Toarcian succession are puzzling because they are not matched by elevated organic carbon burial rates. Both Gill *et al.* (2011) and Newton *et al.* (2011) interpret these data to reflect the presence of low-salinity marine water with low sulphate concentrations. High-latitude water would be a major source of such water, and influx of this water through the Viking Corridor, could perhaps explain this

anomalous signal. Interestingly, $\delta^{34}S_{cas}$ values return to more normal marine values during the Aalenian Age, presumably as the throughflow in the Viking Corridor slowed down or ceased.

Different biotic proxy records show an overall amelioration of oxygen conditions at the sea floor at the Falciferum–Bifrons transition. In Germany this boundary coincides with the deposition of a marker bed known as the Monotis Bed, named after abundant inoceramid bivalves at this level (van de Schootbrugge *et al.* 2018). In southern Germany, prolonged colonization of the sea-floor by benthic bivalves started at this level (Röhl *et al.* 2001), and bioturbation increased in intensity and complexity at this level in the Cleveland Basin (Thibault *et al.* 2018). Ammonites show a high similarity between Arctic and Tethyan faunas during the Falciferum Zone, suggesting faunal exchange proceeded north-wards, driven by global warming. During the Bifrons Zone ammonite faunas became markedly differentiated between high and low latitudes (Dera *et al.* 2011), perhaps indicating isolation of Arctic faunas as a result of predominant southwards flow through the Viking Corridor in addition to increasing latitudinal temperature gradients.

The transition from the Falciferum to the Bifrons Zone marked an end to the most intense anoxic conditions characterized by photic zone euxinia in Germany and the UK. In many southern European Tethyan locations, for example in Italy, Spain and Greece, organic matter accumulation was restricted to this interval in the lower part of the Falciferum (= Serpentinum Zone) and oxygenated conditions were re-established during the remainder of the Toarcian Age. However, in NW-European epeiric sea, deposition of organic-rich sediments continued throughout the Toarcian Age (van de Schootbrugge *et al.* 2018). The prolongation of anoxic conditions in NW Europe for much of the Toarcian Age was likely directly linked to the arrival of low-salinity Arctic waters.

6. Conclusions

The combined use of carbon isotope records and dinoflagellate cyst assemblages from sites within and substantially north and south of the Viking Corridor allow us to shed light on the evolution

of cyst-producing dinoflagellates during early Toarcian time, as well as their migration through the Viking Corridor. The *Parvocysta–Phallocysta* suite of dinoflagellates did not suddenly originate in the Boreal realm during the late Toarcian Age as has been suggested. Instead of being a rapid speciation event, palynological records from Siberia indicate that this important group of characteristic Early Jurassic cyst-forming dinoflagellates originated in the high latitudes in relatively cold Arctic waters, and were able to disperse southwards due to deepening of the Viking Corridor at the end of the Toarcian carbon cycle perturbation at the Falciferum–Bifrons Zone transition (Fig. 12). Arctic origins have also been surmised for other groups of dinoflagellates during the Triassic Period, and could be connected to dynamic nutrient and light conditions in the Arctic. Although the Siberian sections show evidence of black shale deposition, it is likely that conditions were more dynamic here than in lower-latitude sites with frequent mixing and re-oxygenation of the water column in relation to stark seasonal contrasts. This likely explains the high abundance and diversity of dinoflagellate cysts in the Arctic, even at the height of the Toarcian carbon cycle perturbation, much in contrast to NW Europe where a so-called dinoflagellate cyst black-out has been recognized during this interval. The spread of high-latitude phytoplankton following the T-OAE has implications for palaeoceanographic reconstructions for this time interval. Our data reveal that stratification during the T-OAE was not driven by Arctic influx, but rather by increased run-off. Instead, the switch from euxinic conditions to more dysoxic or even oxic conditions in NW Europe and the western Tethys could be explained by the arrival of cooler low-salinity nutrient-rich waters through the Viking Corridor, marking the end of the T-OAE.

References

Ainsworth NR (1986) Toarcian and Aalenian Ostracoda from the Fastnet Basin, offshore South-West Ireland. *Geological Survey of Ireland*, **3**, 277–366.

Al-Suwaidi AH, Angelozzi GN, Baudin F, Damborenea SE, Hesselbo SP, Jenkyns HC, Mancenido MO and Riccardi AC (2010) First record of the Early Toarcian Oceanic Anoxic Event from the Southern Hemisphere, Neuquen Basin, Argentina. *Journal of the Geological Society* **167**, 633–36.

Bailey TR, Rosenthal Y, McArthur JM, van de Schootbrugge B and Thirlwall MF (2003) Paleoceanographic changes of the Late Pliensbachian-Early Toarcian interval: a possible link to the genesis of an Oceanic Anoxic Event. *Earth and Planetary Science Letters* **212**, 307–20.

Bate RH and Coleman BE (1975) Upper Lias Ostracoda from Rutland and Huntingdonshire. *Bulletin of the Geological Survey of Great Britain*, **55**, 1–41.

Bjaerke T (1980) Mesozoic palynology of Svalbard IV. Toarcian dinoflagellates from Spitsbergen. *Palynology* **4**, 57–77.

Bjerrum CJ and Surlyk F (2001) Numerical paleoceanographic study of the Early Jurassic Transcontinental Laurasian seaway. *Paleoceanography* **16**, 390–404.

Bodin S, Krencker FN, Kothe T, Hoffmann R, Mattioli E, Heimhofer U and Kabiri L (2016) Perturbations of the carbon cycle during the late Pliensbachian – early Toarcian: new insight from high-resolution carbon isotope records in Morocco. *Journal of African Earth Sciences* **116**, 89–104.

Bodin S, Mattioli E, Fröhlich S, Marshall JD, Boutib L, Lahsini S and Redfern J (2010) Toarcian carbon isotope shifts and nutrient changes from the northern margin of Gondwana (High Atlas, Morocco, Jurassic): palaeoenvironmental implications. *Palaeogeography, Palaeoclimatology, Palaeoecology* **297**, 377–90.

Boulila S, Galbrun B, Huret E, Hinnov LA, Rouget I, Gardin S and Bartolini A (2014) Astronomical calibration of the Toarcian Stage: implications for sequence stratigraphy and duration of the early Toarcian OAE. *Earth and Planetary Science Letters* **386**, 98–111.

Bucefalo Palliani R, Cirilli S and Mattioli E (1998) Phytoplankton response and geochemical evidence of the lower Toarcian relative sea level rise in the Umbria-Marche Basin (central Italy). *Palaeogeography, Palaeoclimatology, Palaeoecology* **142**, 33–50.

Bucefalo Palliani R, Mattioli E and Riding JB (2002) The response of marine phytoplankton and sedimentary organic matter to the Early Toarcian (Lower Jurassic) oceanic anoxic event in northern England. *Marine Micropaleontology* **46**, 223–45.

Bucefalo Palliani R and Riding JB (1999) Relationships between the early Toarcian anoxic event and organic-walled phytoplankton in central Italy. *Marine Micropaleontology* **37**, 101–16.

Bucefalo Palliani R and Riding JB (2000) A palynological investigation of the Lower and lowermost Middle Jurassic strata (Sinemurian to Aalenian) from North Yorkshire, UK. *Proceedings of the Yorkshire Geological Society* 53, 1–16.

Bujak JP and Fisher MJ (1976) Dinoflagellate cysts from the Upper Triassic of Arctic Canada. *Micropaleontology* **22**, 44–70.

Chamock MA, Kristiansen IL, Ryseth A and Fenton JPG (2001) Sequence stratigraphy of the Lower Jurassic Dunlin Group, northern North Sea. *Norwegian Petroleum Society Special Publications* **10**, 145–74.

Cohen AS, Coe AL, Harding SM and Schwark L (2004) Osmium isotope evidence for the regulation of atmospheric CO2 by continental weathering. *Geology* **32**, 157–60.

Correia VF, Riding JB, Duarte LV, Fernandes P and Pereira Z (2017) The palynological response to the Toarcian Oceanic Anoxic Event (Early Jurassic) at Peniche, Lusitanian Basin, western Portugal. *Marine Micropaleontology* **137**, 46–63.

Da Rocha RB, Mattioli E, Duarte LV, Pittet B, Elmi S, Mouterde R, Cabral MC, Comas-Rengifo MJ, Gomez JJ, Goy A, Hesselbo SP, Jenkyns HC, Littler K, Mailliot S, De Oliveira LCV, Osete ML, Perilli N, Pinto S, Ruget C and Suan G (2016) Base of the Toarcian Stage of the Lower Jurassic defined by the Global Boundary Stratotype Section and Point (GSSP) at the Peniche section (Portugal). *Episodes* **39**, 460.

Davies EH (1983) The dinoflagellate Oppel-zonation of the Jurassic-Lower Cretaceous sequence in the Sverdrup Basin, Arctic Canada. *Geological Survey of Canada Bulletin* **359**, 1–58.

Davies EH (1985) The miospore and dinoflagellate cyst Oppel-zonation of the Lias of Portugal. *Palynology* **9**, 105–32.

Dera G and Donnadieu Y (2012) Modeling evidences for global warming, Arctic seawater freshening, and sluggish oceanic circulation during the Early Toarcian anoxic event. *Paleoceanography* **27**, doi: 10.1029/2012PA002283.

Dera G, Neige P, Dommergues J-L and Brayard A (2011) Ammonite paleobiogeography during the Pliensbachian–Toarcian crisis (Early Jurassic) reflecting paleoclimate, eustasy, and extinctions. *Global and Planetary Change* **78**, 92–105.

Dera G, Pellenard P, Neige P, Deconinck J-F, Puceat E and Dommergues J-L (2009a) Distribution of clay minerals in Early Jurassic Peritethyan seas: palaeoclimatic significance inferred from multiproxy comparisons. *Palaeogeography, Palaeoclimatology, Palaeoecology* **271**, 39–51.

Dera G, Puceat E, Pellenard P, Neige P, Delsate D, Joachimski MM, Reisberg L and Martinez M (2009b) Water mass exchange and variations in seawater temperature in the NW Tethys during the Early Jurassic: evidence from neodymium and oxygen isotopes of fish teeth and belemnites. *Earth and Planetary Science Letters* **286**, 198–207.

Devyatov VP, Knyazev VG and Nikitenko BL (2010) The Pliensbachian–Toarcian boundary of northeastern Siberia and stratigraphic position the Kurung Group of the Kelimyar Formation (Kelimyar River, Olenek River basin). *Otechestvennaya Geologiya* 5, 105–12.

Feist-Burkhardt S and Pross J (2010) Dinoflagellate cyst biostratigraphy of the Opalinuston Formation (Middle Jurassic) in the Aalenian type area in southwest Germany and north Switzerland. *Lethaia* 43, 10–31.

Feist-Burkhardt S and Wille W (1992) Jurassic palynology in southwest Germany – state of the art. *Cahiers de Micropaleontologie* 7, 141–53.

Frimmel A, Oschmann W and Schwark L (2004) Chemostratigraphy of the Posidonia Black Shale, SW Germany I. Influence of sea-level variation on organic facies evolution. *Chemical Geology* 206, 199–230.

Gill BC, Lyons TW and Jenkyns HC (2011) A global perturbation to the sulfur cycle during the Toarcian Oceanic Anoxic Event. *Earth and Planetary Science Letters* 312, 484–96.

Goryacheva AA (2017) Lower Jurassic palynostratigraphy of Eastern Siberia. *Stratigraphy and Geological Correlation* 25, 265–95.

Harazim D, van de Schootbrugge B, Sorichter K, Fiebig J, Weug A, Suan G and Oschmann W (2013) Spatial variability of watermass conditions within the European Epicontinental Seaway during the Early Jurassic (Pliensbachian-Toarcian). *Sedimentology*, published online 21 August 2012, doi: 10.1111/j.1365-3091.2012.01344.x.

Hesselbo SP, Grocke DR, Jenkyns HC, Bjerrum CJ, Farrimond P, Morgans Bell HS and Green OR (2000) Massive dissociation of gas hydrate during a Jurassic oceanic anoxic event. *Nature* 406, 392–95.

Hesselbo SP and Jenkyns HC (1995) A comparison of the Hettangian to Bajocian successions of Dorset and Yorkshire. In *Field Geology of the British Jurassic* (ed. PD Taylor), pp. 105–50. Geological Society of London.

Hesselbo SP, Jenkyns HC, Duarte LV and Oliveira LCV (2007) Carbon isotope record of the Early Jurassic (Toarcian) Oceanic Anoxic Event from fossil wood and marine carbonate (Lusitanian Basin, Portugal). *Earth and Planetary Science Letters* 253, 455–70.

Hesselbo SP and Pienkowski G (2011) Stepwise atmospheric carbon-isotope excursion during the Toarcian Oceanic Anoxic Event (Early Jurassic, Polish Basin). *Earth and Planetary Science Letters* 301, 365–72.

Howard AS (1985) Lithostratigraphy of the Staithes Sandstone and Cleveland Ironstone formations (Lower Jurassic) of north-east Yorkshire. *Proceedings of the Yorkshire Geological Society* 45, 261–75.

Husmo T, Hamar GP, Høiland O, Johannessen EP, Rømuld A, Spencer AM and Bathurst P (2003) Lower and middle Jurassic. In *The Millennium Atlas: Petroleum Geology of the Central and Northern North Sea* (eds D Evans, C Graham, A Armour and P Bathurst), pp. 156. Geological Society of London.

Izumi K, Miyaji T and Tanabe K (2012) Early Toarcian (Early Jurassic) oceanic anoxic event recorded in the shelf deposits in the northwestern Panthalassa: evidence from the Nishinakayama Formation in the Toyora area, west Japan. *Palaeogeography, Palaeoclimatology, Palaeoecology* 315–316, 100–08.

Jenkyns HC (1988) The early Toarcian (Jurassic) anoxic event: stratigraphic, sedimentary, and geochemical evidence. *American Journal of Science* 288, 101–51.

Kafousia N, Karakitsios V, Jenkyns HC and Mattioli E (2011) A global event with a regional character: the Early Toarcian Oceanic Anoxic Event in the Pindos Ocean (northern Peloponnese, Greece). *Geological Magazine* 148, 619–31.

Kemp DB, Coe AL, Cohen AS and Schwark L (2005) Astronomical pacing of methane release in the Early Jurassic period. *Nature* 437, 396–99, doi: 10.1038/nature04037.

Kemp DB, Coe AL, Cohen AS and Weedon GP (2011) Astronomical forcing and chronology of the early Toarcian (Early Jurassic) oceanic anoxic event in Yorkshire, UK. *Paleoceanography* 26, published online 1 November 2011, doi: 10.1029/2011PA002122.

Korte C, Hesselbo SP, Ullmann CV, Dietl G, Ruhl M, Schweigert G and Thibault N (2015) Jurassic climate mode governed by ocean gateway. *Nature Communications* 6, 10015.

Lervik K (2006) Triassic lithostratigraphy of the northern North Sea Basin. *Norsk Geologisk Tidsskrift* 86, 93.

Littler K, Hesselbo SP and Jenkyns HC (2010) A carbon-isotope perturbation at the Pliensbachian-Toarcian boundary: evidence from the Lias Group, NE England. *Geological Magazine* 147, 181–92.

Mangerud G, Paterson NW and Riding JB (2019) The temporal and spatial distribution of Triassic dinoflagellate cysts. *Review of Palaeobotany and Palynology* 261, 53–66.

Martindale RC, Them TR, Gill BC, Marroquín SM and Knoll AH (2017) A new Early Jurassic (ca. 183 Ma) Fossillagerstätte from Ya Ha Tinda, Alberta, Canada. *Geology* 45, 255–58.

McArthur JM, Algeo TJ, van de Schootbrugge B, Li Q and Howarth RJ (2008) Basinal restriction, black shales, Re-Os dating, and the Early Toarcian (Jurassic) oceanic anoxic event. *Paleoceanography* 23, PA4217, doi: 10.1029/2008PA001607.

Montero-Serrano J-C, Föllmi KB, Adatte T, Spangenberg JE, Tribovillard N, Fantasia A and Suan G (2015) Continental weathering and redox conditions during the early Toarcian Oceanic Anoxic Event in the northwestern Tethys: insight from the Posidonia Shale section in the Swiss Jura Mountains. *Palaeogeography, Palaeoclimatology, Palaeoecology* 429, 83–99.

Newton RJ, Reeves EP, Kafousia N, Wignall PB, Bottrell SH and Sha J-G (2011) Low marine sulfate concentrations and the isolation of the European epicontinental sea during the Early Jurassic. *Geology* 39, 7–10.

Nikitenko B, Shurygin B and Mickey MB (2008) High resolution stratigraphy of the Lower Jurassic and Aalenian of Arctic regions as the basis for detailed palaeobiogeographic reconstructions. *Norwegian Journal of Geology* 88, 267–278.

Nikitenko BL (2008) The Early Jurassic to Aalenian Paleobiogeography of the Arctic Realm: implication of Microbenthos (Foraminifers and Ostracodes). *Stratigraphy and Geological Correlation* 16, 59–80.

Nikitenko BL (2009) *Stratigraphy, Paleobiogeography and Biofacies of the Jurassic of Siberia Based on Microfaunas (Foraminifera and Ostracods) [Stratigrafiya, paleobiogeografiya i biofatsii yury Sibiri po mikrofaune (foraminifery i ostrakody)].* Novosibirsk: Parallel, 675 pp. (in Russian with extended English summary).

Nikitenko BL and Mickey MB (2004) Foraminifera and ostracodes across the Pliensbachian–Toarcian boundary in the Arctic Realm (stratigraphy, palaeobiogeography and biofacies). In *The Palynology and Micropalaeontology of Boundaries* (eds AB Beaudoin and MJ Head), pp. 137–174. Geological Society, London, Special Publication no. 230.

Nikitenko BL, Reolid M and Glinskikh L (2013a) Ecostratigraphy of benthic foraminifera for interpreting Arctic record of Early Toarcian biotic crisis (Northern Siberia, Russia). *Palaeogeography, Palaeoclimatology, Palaeoecology* 376, 200–212.

Nikitenko BL and Shurygin BN (1994) Lower Toarcian black shales and Pliensbachian-Toarcian crisis of the biota of Siberian paleoseas. In *Proceedings 1992 International Conference on Arctic Margins, Anchorage, Alaska* (eds DK Thurston and K Fujita), pp. 39–45. US Department of the Interior Minerals Management Service, Alaska Outer Continental Shelf Region, Anchorage, Alaska.

Nikitenko BL, Shurygin BN, Knyazev VG, Meledina SV, Dzyuba OS, Lebedeva NK, Peshchevitskaya EB, Glinskikh LA, Goryacheva AA and Khafaeva CN (2013b) Jurassic and Cretaceous stratigraphy of the Anabar area (Arctic Siberia, Laptev Sea coast) and the boreal zonal standard. *Russian Geology and Geophysics* 54, 808–837.

Ogg JG, Ogg GM0 and Gradstein FM (2016) *A Concise Geologic Time Scale, 2016.* Elsevier, 234 pp.

Poulsen NE (1992) Jurassic dinoflagellate cyst biostratigraphy of the Danish Subbasin in relation to sequences in England and Poland: a preliminary review. *Review of Palaeobotany and Palynology* 75, 33–52.

Poulsen NE and Riding JB (2003) The Jurassic dinoflagellate cyst zonation in Subboreal north-west Europe. In *The Jurassic of Denmark and Greenland* (ed J Ineson). Copenhagen: Geological Survey of Denmark and Greenland, Special Issue.

Prauss M (1989) Dinozysten-Stratigraphie und Palynofazies im oberen Lias und Dogger von NW-Deutschland. *Palaeontographica Abteilung B Band* 214, 1–124.

Prauss M, Ligouis B and Luterbacher H (1991) Organic matter and palyno-morphs in the 'Posidonienschiefer' (Toarcian, Lower Jurassic) of southern Germany. In *Modern and Ancient Continental Shelf Anoxia* (eds RV Tyson and TH Pearson), pp. 335–52. The Geological Society of London.

Prauss M and Riegel W (1989) Evidence of phytoplankton associations for causes of black shale formation in epicontinental seas. *Neues Jahrbuch für Geologie und Paläontologie, Monatshefte* 11, 671–82.

Raucsik B and Varga A (2008) Climate-environmental controls on clay mineral-ogy of the Hettangian-Bajocian successions of the Mecsek Mountains, Hungary: evidence for extreme continental weathering during the Early Toarcian oceanic anoxic event. *Palaeogeography, Palaeoclimatology, Palaeoecology* 265, 1–13.

Riding JB (1984) A palynological investigation of Toarcian to early Aalenian strata from the Blea Wyke area, Ravenscar, North Yorkshire. *Proceeding of the Yorkshire Geological Society* 45, 109–22.

Riding JB, Fedorova VA and Ilyina VI (1999) Jurassic and lowermost Cretaceous dinoflagellate cyst biostratigraphy of the Russian Platform and Northern Siberia, Russia. *AASP Contribution Series* 36, pp. 190.

Riding JB and Ioannides NS (1996) A review of Jurassic dinoflagellate cyst bio-stratigraphy and global provincialism. *Bulletin de la Société géologique de France* 167, 3–14.

Riding JB, Walton W and Shaw D (1991) Toarcian to Bathonian (Jurassic) paly-nology of the Inner Hebrides, Northwest Scotland, *Palynology* 15, 115–179.

Röhl HJ and Schmid-Röhl A (2005) Lower Toarcian (Upper Liassic) black shales of the Central European Epicontinental Basin: A sequence strati-graphic case study from the SW German Posidonia Shale. In *The Deposition of Organic-Carbon-Rich Sediments: Models, Mechanisms and Consequences* (ed. NB Harris) pp. 165–89. SEPM Society for Sedimentary Geology, Special Publication no. 82.

Röhl H-J, Schmid-Röhl A, Oschmann W, Frimmel A and Schwark L (2001) The Posidonia shale (Lower Toarcian) of SW Germany: an oxygen depleted ecosystem controlled by sea level and paleoclimate. *Palaeogeography, Palaeoclimatology, Palaeoecology* 169, 273–99.

Rosales I, Quesada S and Robles S (2004) Paleotemperature variations of Early Jurassic seawater recorded in geochemical trends of belemnites from the Basque-Cantabrian basin, northern Spain. *Palaeogeography, Palaeoclimatology, Palaeoecology* 203, 253–75.

Ruebsam W, Mayer B and Schwark L (2019) Cryosphere carbon dynamics control early Toarcian global warming and sea level evolution. *Global and Planetary Change* 172, 440–53.

Ruebsam W, Muller T, Kovacs J, Palfy J and Schwark L (2018) Environmental response to the early Toarcian carbon cycle and climate perturbations in the northeastern part of the West Tethys shelf. *Gondwana Research* 59, 144–58.

Ruvalcaba Baroni I, Pohl A, van Helmond NAGM, Papadomanolaki NM, Coe AL, Cohen AS, van de Schootbrugge B, Donnadieu Y and Slomp CP (2018) Ocean Circulation in the Toarcian (Early Jurassic): a Key Control on Deoxygenation and Carbon Burial on the European Shelf. *Paleoceanography and Paleoclimatology* 33, 994–1012.

Sabatino N, Neri R, Bellanca A, Jenkyns HC, Baudin F, Parisi G and Masetti D (2009) Carbon isotope records of the Early Jurassic (Toarcian) oceanic anoxic event from the Valdorbia (Umbria-Marche Apennines) and Monte Mangart (Julian Alps) sections: palaeoceanographic and stratigraphic impli-cations. *Sedimentology* 56, 1307–28.

Sabatino N, Vlahovic I, Jenkyns HC, Scopelliti G, Neri R, Prtoljan B and Velic IVO (2013) Carbon-isotope record and palaeoenvironmental changes during the early Toarcian oceanic anoxic event in shallow-marine carbonates of the Adriatic Carbonate Platform in Croatia. *Geological Magazine* 150, 1085–102.

Schouten S, Kaam-Peters HME, van Schoell M and Sinninghe Damsté JS (2000) Effects of an oceanic anoxic event on the stable carbon isotopic com-position of Early Toarcian carbon. *American Journal of Science* 300, 1–22.

Scotese CR (2016) PALEOMAP PaleoAtlas for GPlates and the PaleoData Plotter Program. PALEOMAP Project. Technical Report, doi: 10.13140/RG.2.2.34367.00166.

Simms MJ, Chidlaw N, Morton N and Page KN (2004) *British Lower Jurassic Stratigraphy*. Peterborough: Joint Nature Conservation Committee.

Steel RJ (1993) Triassic–Jurassic megasequence stratigraphy in the Northern North Sea: Rift to post-rift evolution. In *Geological Society of London, Petroleum Geology Conference series no. 4*. pp. 299–315.

Suan G, Mattioli E, Pittet B, Mailliot S and Lecuyer C (2008a) Evidence for major environmental perturbation prior to and during the Toarcian (Early Jurassic) oceanic anoxic event from the Lusitanian Basin, Portugal. *Paleoceanography* 23, PA1202, doi: 10.029/2007PA001459.

Suan G, Nikitenko BL, Rogov MA, Baudin F, Spangenberg JE, Knyazev VG, Glinskikh LA, Goryacheva AA, Adatte T, Riding JB, Föllmi KB, Pittet B, Mattioli E and Lecuyer C (2011) Polar record of Early Jurassic massive car-bon injection. *Earth and Planetary Science Letters* 312, 102–13.

Suan G, Pittet B, Bour I, Mattioli E, Duarte LV and Mailliot S (2008b) Duration of the Early Toarcian carbon isotope excursion deduced from spec-tral analysis: consequence for its possible causes. *Earth and Planetary Science Letters* 267, 666–679.

Suan G, van de Schootbrugge B, Adatte T, Fiebig J and Oschmann W (2015) Calibrating the magnitude of the Toarcian carbon cycle perturbation. *Paleoceanography* 30, 495–509.

Them TR, Gill BC, Selby D, Grocke DR, Friedman RM and Owens JD (2017) Evidence for rapid weathering response to climatic warming during the Toarcian Oceanic Anoxic Event. *Scientific Reports* 7, 5003.

Thibault N, Ruhl M, Ullmann CV, Korte C, Kemp DB, Gröcke DR and Hesselbo SP (2018) The wider context of the Lower Jurassic Toarcian oce-anic anoxic event in Yorkshire coastal outcrops, UK. *Proceedings of the Geologists' Association* 129, 372–91.

Triebel E (1950) Camptocythere, eine neue Ostracoden-Gattung aus dem Dogger Norddeutschlands. *Senckenbergiana* 31, 197–208.

van de Schootbrugge B, Bachan A, Suan G, Richoz S and Payne JL (2013) Microbes, mud and methane: cause and consequence of recurrent Early Jurassic anoxia following the End-Triassic mass extinction. *Palaeontology* 56, 685–709.

van de Schootbrugge B, MacArthur JM, Baily TR, Rosenthal Y, Wright JD and Miller KG (2005) Toarcian oceanic anoxic event: assessment of global causes using belemnite C-isotope records. *Paleoceanography and Palaeoclimatology* 20, published online 26 August 2005, doi: 10.1029/2004PA001102.

van de Schootbrugge B, Payne JL, Tomasovych A, Pross J, Fiebig J, Benbrahim M, Föllmi KB and Quan TM (2008) Carbon cycle perturba-tion and stabilization in the wake of the Triassic-Jurassic boundary mass-extinction event. *Geochemistry, Geophysics, Geosystems* 9, Q04028, doi: 10.1029/2007GC001914.

van de Schootbrugge B, Richoz S, Pross J, Luppold FW, Hunze S, Wonik T, Blau T, Meister C, van der Weijst CMH, Suan G, Fraguas A, Fiebig J, Herrle JO, Guex J, Little CTS, Wignall PB, Püttmann W and Oschmann W (2018). The Schandelah Scientific Drilling Project: a 25-mil-lion year record of Early Jurassic palaeo-environmental change from northern Germany. *Newsletters on Stratigraphy* 52(3), 249–96.

van Helmond NAGM, Sluijs A, Papadomanolaki NM, Plint AG, Gröcke DR, Pearce MA, Eldrett JS, Trabucho-Alexandre J, Walaszczyk I, van de Schootbrugge B and Brinkhuis H (2016) Equatorward phytoplankton migration during a cold spell within the Late Cretaceous super-greenhouse. *Biogeosciences* 13, 2859–72.

Vellekoop J, Smit J, van de Schootbrugge B, Weijers JWH, Galeotti S, Sinninghe Damsté JS and Brinkhuis H (2015) Palynological evidence for prolonged cooling along the Tunisian continental shelf following the K–Pg boundary impact. *Palaeogeography, Palaeoclimatology, Palaeoecology* 426, 216–28.

Vollset J and Doré AG (eds) (1984) *A revised Triassic and Jurassic Lithostratigraphic Nomenclature for the Norwegian North Sea*. Stavanger: Olijedirektoratet.

Wiggan NJ, Riding JB, Fensome RA and Mattioli E (2018) The Bajocian (Middle Jurassic): a key interval in the early Mesozoic phytoplankton radi-ation. *Earth-Science Reviews* 180, 126–46.

Wiggins VD (1973) Upper Triassic dinoflagellates from arctic Alaska. *Micropaleontology* 19, 1–16.

Wiggins VD (1978) Upper Triassic-Lower Jurassic dinoflagellates. *Palynology* **2**, 236.

Wille W (1982) Evolution and ecology of Upper Liassic dinoflagellates from SW Germany. *Neues Jahrbuch für Geologie und Paläontologie, Abhandlungen* **164**, 74–82.

Xu W, Ruhl M, Jenkyns HC, Leng MJ, Huggett JM, Minisini D, Ullmann CV, Riding JB, Weijers JWH, Storm MS, Percival LME, Tosca NJ, Idiz EF, Tegelaar EW and Hesselbo SP (2018) Evolution of the Toarcian (Early Jurassic) carbon-cycle and global climatic controls on local sedimentary processes (Cardigan Bay Basin, UK). *Earth and Planetary Science Letters* **484**, 396–411.

Zakharov VA, Shurygin BN, Il'ina VI and Nikitenko BL (2006) Pliensbachian-Toarcian biotic turnover in north Siberia and the Arctic region. *Stratigraphy and Geological Correlation* **14**, 399–417.

Zavattieri AM, Rosenfeld U and Volkheimer W (2008) Palynofacies analysis and sedimentary environment of Early Jurassic coastal sediments at the southern border of the Neuquén Basin, Argentina. *Journal of South American Earth Sciences* **25**, 227–45.